PROPAGATION OF LIGHT IN QUADRATIC INDEX PROFILE WAVEGUIDES

by

NEIL APORONGAO REBOLLEDO

B.S., Metropolitan State College of Denver, 2006

A thesis submitted to the

Faculty of the Graduate School of the

University of Colorado in partial fulfillment

of the requirements for the degree of

Master of Integrated Sciences

Integrated Sciences Program

2015

This thesis for the Master of Integrated Sciences degree by

Neil Aporongao Rebolledo

has been approved for the

Integrated Sciences Program

by

Randall P. Tagg, Chair

Masoud Asadi-Zeydabadi

Burt Simon

Date: April 24, 2015

Rebolledo, Neil Aporongao (M.I.S., Integrated Sciences)

Propagation of Light in Quadratic Index Profile Waveguides

Thesis directed by Associate Professor Randall P. Tagg.

ABSTRACT

Optical gradient index media have the property where the spatial variation of the index of refraction is continuous along the direction transverse to the optical axis. Many emerging technologies in optics require gradient index components, and a firm understanding of the physics of light propagation in these components is required. Presented here are the mathematical foundations used to analyze light propagation in planar quadratic index profile waveguides. One transverse direction is used in this analysis, and light propagation is seen to have periodic behavior. Also presented here is a comparison of ray bundles and wave intensities in quadratic index waveguides, with the intent to use this machinery to further ray chaos theory.

The form and content of this abstract are approved. I recommend its publication.

Approved: Randall P. Tagg

For Cécile, Luna, Boo Bear, Liwan, Winnie, and Colette.

ACKNOWLEDGEMENTS

Many thanks and sincere gratitude to my thesis committee members Dr. Randall Tagg, Dr. Masoud Asadi-Zeydabadi, and Dr. Burt Simon. They have been extremely supportive throughout this thesis project, working around my work schedule to setup our meetings, answering questions over the phone, responding to late night and early morning emails, and have given me invaluable advice and guidance that I will take with me for the rest of my career. Many many thanks also goes out to Dr. Martin Huber, who I first met as my undergraduate senior lab professor (the same time I met Masoud, who at the time was assisting Martin with his upper division lab courses), and now as my program director for this degree. Your time, effort, and support as my program adviser at UC Denver is very much appreciated, and I cannot thank you enough for helping me as a graduate student in your masters degree program.

Acknowledgement also goes out to the physics department at the University of Colorado Colorado Springs, especially to Dr. Robert Camley, Dr. Zbigniew Celinski, and Dr. Anatoliy Glushchenko. They supported me as a physics graduate student, and supported my decision to transfer to UC Denver. Special thanks to my friends Seth Johnson, Scott Davis, Juan Pino, George Farca, Scott Rommel, and Michael Anderson, who I all met while working at Vescent Photonics. They gave me my start in optical physics, gave me the boost I needed to succeed in science and engineering, and were very supportive of my pursuit of a masters degree. And a very special thank you to Cotton Anderson who I met while working at Research Electro-Optics. He furthered my professional exposure in optics, data collection and analysis, and showed me software writing techniques that I later used to write the scripts for this thesis project.

My sincere gratitude also goes out to Dr. Richard Krantz who supported my pursuit of a masters degree from the start by writing a letter of recommendation for admission into the physics graduate program at UCCS. Dr. Krantz was my very first undergraduate physics professor, and he also supervised my undergraduate capstone project in mathematical music theory. It was during this time where I got my first exposure to scientific programming, collaborating and testing ideas, and presenting my results. These skills prepared me for

both my professional and academic endeavors. It has also been a real pleasure running into him on campus as I complete my master's degree, catching up, and telling him about my thesis project. Thank you Dr. K.!

TABLE OF CONTENTS

CHAPTER

LIST OF FIGURES

FIGURES

CHAPTER I

WHY STUDY QUADRATIC INDEX WAVEGUIDES?

That question alone contains so much information that if one doesn't know the meaning of any of the words *quadratic, index,* or *waveguide*, then the question *"why study quadratic index waveguides?"* only has one answer, *"I'd rather not."* But if one does understand the question, and wishes for some reason to read further, then what's presented here as an attempt to answer the title of this section will hopefully be informative, if not profound.

Quadratic index waveguides are devices that have an index of refraction that is spatially varying perpendicular to the optical axis. This variation is quadratically decreasing to the boundary from the center of the waveguide. Waveguides and optical devices that have this feature are fundamental to the advancement of technologies such as optical communications, laser systems, and photonic integrated circuits. A thorough understanding of quadratic index waveguides is also fundamental to problems involving chaotic ray behavior, and light propagation in geometries with regular inhomogeneities in the axial direction. The mathematical formulations used to describe light propagation in quadratic index waveguides can also be used to describe other types of wave propagation, such as acoustic and ocean waves.

There are two approaches to analyzing light propagation in quadratic index waveguides. One approach is to assume that the dimensions of the waveguide are much larger than the wavelength of the incident light. We then only need to consider the propagation direction of the energy of the wavefronts, and we can model light as *rays*. This is called the *geometric optics* treatment of light propagation. This approach to analyzing light propagation in quadratic index waveguides has a remarkable connection to a physically different system, the classical harmonic oscillator. That connection lies in the mathematics based on the Hamiltonian formulation of particle dynamics. The Hamiltonian formulation uses a set of first-order differential equations, called Hamilton's Equations, to describe particle trajectories subject to a force, and when applied to the classical harmonic oscillator, we obtain analytic solutions that describe periodic, sinusoidal particle trajectories. When Hamilton's equations are applied to light propagation in quadratic index waveguides, we can think of the index profile as the 'force'. After solving Hamilton's Equations, we obtain analytic solutions

for ray trajectories in quadratic index waveguides, and the ray trajectories are shown to be sinusoidal [2],[3],[6],[10]. The existence of the connection between ray paths in quadratic index waveguides, and particle trajectories for the classical harmonic oscillator shows that two physically different systems are described by the same mathematics.

The other approach to analyzing light propagation in quadratic index waveguides is to assume that the dimensions of the waveguide are of the same length scale as the wavelength of the incident light. The wavelength now matters, something that is ignored in the geometric optics approach, and we now need to define quantities that will help describe the waves interaction with the geometry of our analysis. This approach is called the *wave optics* treatment of light propagation. Light propagation in quadratic index waveguides is described by solving the Helmholtz wave equation, which is based upon Maxwell's Equations. The wave optics treatment of light propagation of our problem has a mathematical connection to the quantum harmonic oscillator. Solutions to the quantum harmonic oscillator are found by solving the Schrodinger Equation, and an exact solution can be found that will specify the energy-levels. The solutions found are a complete set of solutions based upon the Hermite polynomials. The solutions to the Helmholtz wave equation is also a complete set of solutions based upon the Hermite polynomials. Again we see two physically different systems related by the same mathematics. This thesis aims to not only show the geometric and wave optics treatment of light propagation in quadratic index waveguides, but to also show how mathematics, the language of physics, connects systems that are physically different.

So what is a quadratic index profile? In this thesis, the mathematical expression for the refractive index profile is of the form

$$n^2(x) = n_0^2 - (n_0^2 - n_1^2)\frac{x^2}{a_0^2} \tag{1}$$

where n_o is the maximum value at the center of the waveguide, and decreases quadratically to n_1 at the boundary. The quantity a_o is the distance from center of the waveguide, or the waveguide half-width. The index profile (1) was chosen so that n_0 and n_1 are dimensionless, and units of length are canceled by the factor x^2/a_0^2. Equation (1) is one example of a quadratic (or gradient) refractive index profile. One example of practical devices that utilizes

this type of index profile are gradient-index (GRIN) optics [13]. GRIN optics are discrete optical components behaving like lenses that have, similar to quadratic-index waveguides, a varying index of refraction in the radial direction. These optics have been used to reduce aberrations in imaging systems, to reduce cost and weight in optical assemblies, and to produce collimated optical fibers. Another gradient-index device application is the gradient-index fiber. The index of refraction of the core decreases with radial distance from the optical axis, and these fiber optics are used in optical communications applications for their capability of guiding light over large distances [5].

The advancement of integrated photonics is increasingly becoming more reliant on optical components that have a spatially varying index of refraction. It is becoming increasingly desired to integrate conventional optics with GRIN-like optics to reduce cost and weight of integrated photonic systems [15].

How Do We Simulate Light Propagation In Quadratic Index Waveguides?

Lets take a closer look at the two approaches to analyzing light propagation in quadratic index waveguides. First the geometric optics treatment. This approach uses Hamilton's Equations which are first-order differential equations that couple the ray's position and momentum. When Hamilton's Equations are solved for light propagation in quadratic index waveguides, they yield expressions that show ray paths propagate sinusoidally. The techniques of *ray tracing* can be used to simulate this light propagation [1], [8]. The software tool used in this thesis to simulate ray paths is Octave, a MatLab clone. An Octave script can be written to define the waveguide dimensions and refractive indices, and the exact solutions from Hamilton's equations can be coded as well. Built-in plotting functions native to Octave can then be used to create plots showing ray paths in our system. We can solve Hamilton's Equations directly by using a differential equation solver function native to Octave (and Matlab) called `ode45`. This function uses an iterative Runge-Kutta approximation to directly solve Hamilton's equations. This numerical approach can be compared to the exact solutions to Hamilton's equations, and it will be seen here to be in excellent agreement with each other.

The wave optics treatment of light propagation in quadratic index waveguides requires us

to solve the Helmholtz wave equation, which is a second-order partial differential equation whose solution represents any component of the wave. For the analysis in this thesis, a Gaussian distribution is initially at the left boundary of the waveguide, and is expanded in terms of the Hermite polynomials to solve the Helmholtz wave equation. The analytic solution for the field profile is seen to have a periodic behavior. Octave was also used to simulate wave propagation in quadratic index waveguides from the analytic solution to the Helmholtz equation. The numerical software tool used to simulate wave propagation is *MEEP* [12], which utilizes the *finite difference time domain* (FDTD) method to solve Maxwell's Equations by discretizing space and time into regular rectangular grids [14]. The electric and magnetic fields are calculated at appropriate grid locations, and the state of the wave at any time step is based on the state of the wave at the previous time step. This method is a popular choice for computational electromagnetic problems because of the balance between computing requirements and accuracy. MEEP simulations are also performed by first writing a script defining the computational cell size, refractive indices, and initial Gaussian distribution at the left boundary. A comparison of the wave intensities from the analytic solution to the MEEP simulations is also shown in this thesis.

Putting It All Together, And Where To Go From Here?

One goal of this thesis is to show that if we know how rays propagate in quadratic index waveguides, we can then accurately predict the corresponding wave behavior, and vice-versa. The validity of the numerical approaches used for the geometric and wave optics treatment is reinforced by comparing each approach to known analytical solutions. This will create a foundation to extend the numerical approaches to situations where analytical solutions to the ray and wave treatments are no longer viable. Of special interest is the introduction of axial modulation of the index of refraction. Such a system has been shown to generate chaotic ray paths, and it is of interest to know how this translates into intensity variations of light in actual systems. Thus, a numerical scheme to relate intensity profiles obtained from the wave optics treatment to the concentration of bundles of trajectories from ray tracing techniques is strongly desired.

Such a validated approach will be useful for fundamental studies of chaotic propagation in

axially modulated waveguides and will also be of great practical value in describing systems in which light propagates through periodic structures whose scale of variation is larger than the wavelength of light but not large enough to ignore the wave nature of light. An example is media composed of regularly spaced living cells in which the nuclei creates a periodic variation of the index of refraction.

CHAPTER II

ELECTROMAGNETICS AND GEOMETRIC OPTICS

In physics we think of light as electromagnetic waves, the same kind of waves you would see propagating in water. These electromagnetic waves are what we believe cause the perception of light. A general mathematical expression that describes the motion of these waves is

$$f(z,t) = f(z - vt, 0) = g(z - vt) \tag{2}$$

This equation describes the displacement of a wave a distance z at time t. Electromagnetic waves are analogous to waves produced on a string that shakes up and down. These kinds of waves are called transverse waves. By using Newton's second law, $F = m\frac{d^2x}{dt^2}$, on a segment of the string which has a tension T on both ends as it is displaced from its equilibrium position, the string will experience a force in the transverse direction between z and $z + \delta z$

$$\Delta F \cong T(\frac{\partial f}{\partial z}|_{z+\Delta z}) - \frac{\partial f}{\partial z}|_z) \cong T\frac{\partial^2 f}{\partial z^2} \tag{3}$$

If μ is the mass per unit length, Newton's second law for this system is $\Delta F = \mu(\Delta z)\frac{\partial^2 f}{\partial t^2}$, and equating this with (3) gives

$$\frac{\partial^2 f}{\partial z^2} = \frac{\mu}{T}\frac{\partial^2 f}{\partial t^2}. \tag{4}$$

and for small disturbances

$$\frac{\partial^2 f}{\partial z^2} = \frac{1}{v^2}\frac{\partial^2 f}{\partial t^2} \tag{5}$$

where v is the speed of propagation of the wave, and equal to $\sqrt{\frac{T}{\mu}}$. Equation (5) is the classical wave equation in one dimension, and has solutions of the form

$$f(z,t) = g(z - vt). \tag{6}$$

Electromagnetic Waves

Electromagnetic waves are most often represented as sinusoidal waves

$$f(z,t) = A\cos[k(z-vt)+\delta]. \tag{7}$$

The argument of cos is the phase of the wave, δ is the phase constant which has values between $0 \leq \delta \leq 2\pi$, and k is the wave number of the wave and is related to the wavelength λ by

$$k = \frac{2\pi}{\lambda}. \tag{8}$$

The wave number is the number of cycles per unit distance, or number of waves per unit distance. When the wave travels a distance of one wavelength $\lambda = \frac{2\pi}{k}$, the cosine executes one complete cycle. At any fixed point z, the string vibrates up and down and completes one cycle in a period T

$$T = \frac{2\pi}{kv}. \tag{9}$$

The period is related to the frequency ν (number of oscillations per unit time) by

$$\nu = \frac{1}{T} = \frac{kv}{2\pi} = \frac{v}{\lambda}. \tag{10}$$

Sinusoidal waves can be written in terms of the angular frequency $\omega = 2\pi\nu = kv$, the number of radians swept out per unit time. The expression for sinusoidal waves is of the form

$$f(z,t) = A\cos(kz-\omega t+\delta). \tag{11}$$

Using Euler's formula, $e^{i\theta} = \cos\theta + i\sin\theta$, sinusoidal waves can be expressed in complex notation

$$\tilde{f}(z,t) = \tilde{A}e^{i(kz-\omega t)} \tag{12}$$

where the complex amplitude is $\tilde{A} = Ae^{i\delta}$.

Any wave can be expressed as a linear combination of sinusoidal waves

$$\tilde{f}(z,t) = \int_{-\infty}^{+\infty} \tilde{A}(k) e^{i(kz-\omega t)} dk. \tag{13}$$

Equation (13) shows that any wave can be written as a linear combination of sinusoidal waves, and if we know the behavior of sinusoidal waves, we then know the behavior of any types of waves.

Reflection and Transmission of Waves

Consider a sinusoidal wave incident on the xy plane arriving from the left. Immediately after the incident wave interacts with the xy plane, a reflected wave is produced and travels in the opposite direction of the incident wave. At the same time, a transmitted wave is produced on the right side of the xy plane, and travels in the same direction as the incident wave. The reflected and transmitted wave may have the same speed of propagation as the incident wave, or the transmitted wave may have a different speed of propagation if it is in a different medium. Taking z as the propagation direction, these waves are mathematically represented as

$$\tilde{f}_I(z,t) = \tilde{A}_I e^{i(k_1 z-\omega t)}, \text{ for } z < 0 \tag{14}$$

$$\tilde{f}_R(z,t) = \tilde{A_R} e^{i(-k_1 z-\omega t)}, \text{ for } z < 0 \tag{15}$$

$$\tilde{f}_T(z,t) = \tilde{A_T} e^{i(k_2 z-\omega t)}, \text{ for } z > 0 \tag{16}$$

The displacement of the wave just to the left and right of the xy plane must be the same, $f(0^-,t) = f(0^+,t)$. Assuming the xy plane interface has negligible mass, then the derivative of f is also continuous, $\frac{\partial f}{\partial z}_{0^-} = \frac{\partial f}{\partial z}_{0^+}$.

Polarization

As stated earlier, electromagnetic waves are transverse waves, and the displacement of these types of waves is perpendicular to the direction of propagation. Electromagnetic waves have two quantities whose displacement is perpendicular to the propagation direction, and can then have two states of polarization. Analogous to shaking a string, you can shake

it horizontally or vertically. For example, for a wave polarized in the $\hat{\mathbf{x}}$ direction we have $\tilde{\mathbf{f}}(z,t) = \tilde{A}e^{i(kz-\omega t)}\hat{\mathbf{x}}$, and for a wave polarized in the $\hat{\mathbf{y}}$ direction $\tilde{\mathbf{f}}(z,t) = \tilde{A}e^{i(kz-\omega t)}\hat{\mathbf{y}}$. In general

$$\tilde{\mathbf{f}}(z,t) = \tilde{A}e^{i(kz-\omega t)}\hat{\mathbf{n}}. \tag{17}$$

The polarization vector $\hat{\mathbf{n}}$ defines the plane of vibration, and since this plane is perpendicular to the direction of propagation $\hat{\mathbf{n}} \cdot \hat{\mathbf{z}} = 0$, and $\hat{\mathbf{n}} = \cos\theta\hat{\mathbf{x}} + \sin\theta\hat{\mathbf{y}}$. So a wave can be described as a superposition of two waves, each wave in one of the states of polarization

$$\tilde{\mathbf{f}}(z,t) = (\tilde{A}\cos\theta)e^{i(kz-\omega t)}\hat{\mathbf{x}} + (\tilde{A}\sin\theta)e^{i(kz-\omega t)}\hat{\mathbf{y}}. \tag{18}$$

Plane Waves

Sinusoidal waves traveling in the z direction and have no x and y dependence are called plane waves. Plane waves have uniform fields over every plane perpendicular to the direction of propagation. The expressions for plane waves for electric and magnetic fields in a vacuum are

$$\tilde{\mathbf{E}}(z,t) = \tilde{\mathbf{E}}_0 e^{i(kz-\omega t)} \tag{19}$$

$$\tilde{\mathbf{B}}(z,t) = \tilde{\mathbf{B}}_0 e^{i(kz-\omega t)}. \tag{20}$$

These are also solutions to Maxwell's equations in a charge free, and current free medium. $\tilde{\mathbf{E}}_0$ and $\tilde{\mathbf{B}}_0$ are the complex amplitudes. Over small enough regions, any wave is a plane wave, as long as its wavelength is much less than the radius of the curvature of the wavefront.

We can generalize the propagation direction kz to any direction $\mathbf{r}$, and by introducing the wave vector $\mathbf{k}$, which points in the direction of propagation.

$$\tilde{\mathbf{E}}(\mathbf{r},t) = \tilde{E}_0 e^{i(\mathbf{k}\cdot\mathbf{r}-\omega t)}\hat{\mathbf{n}} \tag{21}$$

$$\tilde{\mathbf{B}}(\mathbf{r},t) = \tilde{B}_0 e^{i(\mathbf{k}\cdot\mathbf{r}-\omega t)}\hat{\mathbf{n}} \tag{22}$$

Energy and Momentum in Electromagnetic Waves

The energy per unit time in an electromagnetic field is

$$u = \frac{1}{2}\left(\epsilon_0 E^2 + \frac{1}{\mu_0} B^2\right) \tag{23}$$

where ϵ_0 is the permitivity of free space, μ_0 is the permeability of free space. The energy densities for the electric field is $u_E = \frac{1}{2}\epsilon_0 E^2$, and $u_B = \frac{B^2}{2\mu_0}$ for the magnetic field. For monochromatic plane waves, $B^2 = \frac{1}{c^2}E^2 = \mu_0\epsilon_0 E^2$, so the electric and magnetic field contributions are equal

$$u = \epsilon_0 E^2 = \epsilon_0 E_0^2 \cos^2(kz - \omega t + \delta). \tag{24}$$

The energy flux density, or energy per unit area, per unit time, is given by the Poynting vector

$$\mathbf{S} = \frac{1}{\mu_0}(\mathbf{E} \times \mathbf{B}) \tag{25}$$

and for monochromatic plane waves in the z direction

$$\mathbf{S} = c\epsilon_0 E^2 \cos^2(kz - \omega t + \delta)\hat{\mathbf{z}} = cu\hat{\mathbf{z}} \tag{26}$$

so that $\mathbf{S}$ is the energy density u times the velocity of the wave $c\hat{\mathbf{z}}$.

Electromagnetic fields also carry momentum, and the momentum density stored in the field is

$$\wp = \frac{1}{c^2}\mathbf{S} \tag{27}$$

and for monochromatic plane waves

$$\wp = \frac{1}{c^2}\epsilon_0 E^2 \cos^2(kz - \omega t + \delta)\hat{\mathbf{z}} = \frac{1}{c}u\hat{\mathbf{z}} \tag{28}$$

$$\langle u \rangle = \frac{1}{2}\epsilon_0 E^2 \tag{29}$$

$$\langle \mathbf{S} \rangle = \frac{1}{2}c\epsilon_0 E^2 \hat{\mathbf{z}} \tag{30}$$

$$\langle \wp \rangle = \frac{1}{2c}\epsilon_0 E_0^2 \hat{\mathbf{z}} \tag{31}$$

The brackets represent the time average over a complete cycle, or many cycles. The average power per unit area transported by an electromagnetic wave is the intensity

$$\boldsymbol{I} \equiv \langle S \rangle = \frac{1}{2} c \epsilon_0 E_0^2 \tag{32}$$

Light can impart momentum on a surface if the material is a perfect absorber in a time interval Δt the momentum transfer is $\Delta \mathbf{p} = \langle \wp \rangle \, Ac\Delta t$, so the radiation pressure (average force per unit area) is

$$P = \frac{1}{A}\frac{\Delta p}{\Delta t} = \frac{1}{2}\epsilon_0 E_0^2 = \frac{1}{c} \tag{33}$$

Maxwell's Equations

In a charge free and current free space, Maxwell's equations are

$$\nabla \cdot \mathbf{E} = 0 \tag{34}$$

$$\nabla \cdot \mathbf{B} = 0 \tag{35}$$

$$\nabla \times \mathbf{E} = -\frac{\partial \mathbf{B}}{\partial t} \tag{36}$$

$$\nabla \times \mathbf{B} = \mu_0 \epsilon_0 \frac{\partial \mathbf{E}}{\partial t} \tag{37}$$

These equations are coupled, first-order partial differential equations for $\mathbf{E}$ and $\mathbf{B}$. They can be decoupled by taking the curl of the curl equations

$$\nabla \times (\nabla \times \mathbf{E}) = \nabla (\nabla \cdot \mathbf{E}) - \nabla^2 \mathbf{E} = \nabla \times \left(-\frac{\partial \mathbf{B}}{\partial t} \right) = -\frac{\partial}{\partial t} (\nabla \times \mathbf{B}) = -\mu_0 \epsilon_0 \frac{\partial^2 \mathbf{E}}{\partial t^2} \tag{38}$$

$$\nabla \times (\nabla \times \mathbf{B}) = \nabla (\nabla \cdot \mathbf{B}) - \nabla^2 \mathbf{B} = \nabla \times \left(-\frac{\partial \mathbf{E}}{\partial t} \right) = -\frac{\partial}{\partial t} (\nabla \times \mathbf{E}) = -\mu_0 \epsilon_0 \frac{\partial^2 \mathbf{B}}{\partial t^2}. \tag{39}$$

Using the divergence equations (34) and (35), (38) and (39) become

$$\nabla^2 \mathbf{E} = \mu_0 \epsilon_0 \frac{\partial^2 \mathbf{E}}{\partial t^2} \tag{40}$$

$$\nabla^2 \mathbf{B} = \mu_0 \epsilon_0 \frac{\partial^2 \mathbf{B}}{\partial t^2} \tag{41}$$

which are the wave equations for the electric and magnetic fields derived from Maxwell's equations in a vacuum. What started as coupled first-order partial differential equations are not separate second-order partial differential equations.

Faraday's Law (36) gives a relation between the amplitudes of the electric and magnetic fields

$$-k(\tilde{E}_0)_y = \omega(\tilde{B}_0)_x$$

and

$$k(\tilde{E}_0)_x = \omega(\tilde{B}_0)_y.$$

These results can be generalized as

$$\tilde{\mathbf{B}}_0 = \frac{k}{\omega}(\hat{\mathbf{z}} \times \tilde{\mathbf{E}}_0). \tag{42}$$

We then also have a relation between their real amplitudes

$$B_0 = \frac{k}{\omega}E_0 = \frac{1}{c}E_0. \tag{43}$$

so that (22) becomes

$$\tilde{\mathbf{B}}(\mathbf{r}, t) = \frac{1}{c}(\hat{\mathbf{k}} \times \tilde{\mathbf{E}}) \tag{44}$$

Maxwell's Equations in Linear Media

Consider matter that allows for electromagnetic wave propagation, and is free from charge and current. The electric displacement and auxiliary magnetic field due to the material are

$$\mathbf{D} = \epsilon\mathbf{E} \tag{45}$$

$$\mathbf{H} = \frac{1}{\mu}\mathbf{B} \tag{46}$$

where ϵ is the permitivity of the material, and μ is the permeability of the material. Maxwell's equations for linear matter then become

$$\nabla \cdot \mathbf{D} = 0 \tag{47}$$

$$\nabla \cdot \mathbf{B} = 0 \tag{48}$$

$$\nabla \times \mathbf{E} = -\frac{\partial \mathbf{B}}{\partial t} \tag{49}$$

$$\nabla \times \mathbf{H} = \frac{\partial \mathbf{D}}{\partial t} \tag{50}$$

In a homogeneous medium, ϵ and μ do not vary from point to point. Maxwell's equations then reduce to

$$\nabla \cdot \mathbf{E} = 0 \tag{51}$$

$$\nabla \cdot \mathbf{B} = 0 \tag{52}$$

$$\nabla \times \mathbf{E} = -\frac{\partial \mathbf{B}}{\partial t} \tag{53}$$

$$\nabla \times \mathbf{B} = \mu\epsilon \frac{\partial \mathbf{E}}{\partial t} \tag{54}$$

The speed of propagation of an electromagnetic wave in a linear homogeneous medium is $v = \frac{1}{\sqrt{\mu\epsilon}} = \frac{c}{n}$, where $n = \sqrt{\frac{\mu\epsilon}{\mu_0\epsilon_0}}$ is the index of refraction. It is the ratio between the speed of propagation of electromagnetic waves in the medium and in a vacuum. For most materials, $\mu \approx \mu_0$, therefore $n \simeq \sqrt{\epsilon_r}$ where ϵ_r is the dielectric constant of the material. Since ϵ_r is always greater and 1, light travels more slowly through matter.

Wave equations for $\mathbf{E}$ and $\mathbf{B}$ in linear media can be obtained by the same procedure that yielded the wave equations (40) and (41)

$$\nabla^2 \mathbf{E} = \mu\epsilon \frac{\partial^2 \mathbf{E}}{\partial t^2} \tag{55}$$

$$\nabla^2 \mathbf{B} = \mu\epsilon \frac{\partial^2 \mathbf{B}}{\partial t^2}. \tag{56}$$

Looking just at the wave equation for $\mathbf{E}$, which holds for all components of $\mathbf{E}$, and is equivalent to saying that all components of $\mathbf{E}$ also satisfy the scalar wave equation

$$\nabla^2 \psi = \frac{1}{v^2} \frac{\partial^2 \psi}{\partial t^2}. \tag{57}$$

where $v = 1/(\mu\epsilon)^{1/2}$. This describes interference and diffraction effects of the wave, and ψ

can represent any component of $\mathbf{E}$.

Boundary Conditions

Consider an electromagnetic wave interacting with an interface. The wave obeys the following boundary conditions

$$\epsilon_1 E_1^{\perp} = \epsilon_2 E_2^{\perp} \tag{58}$$

$$B_1^{\perp} = B_2^{\perp} \tag{59}$$

$$\mathbf{E}_1^{\parallel} = \mathbf{E}_2^{\parallel} \tag{60}$$

$$\frac{1}{\mu_1}\mathbf{B}_1^{\parallel} = \frac{1}{\mu_2}\mathbf{B}_2^{\parallel} \tag{61}$$

These equations relate the electric and magnetic fields just to the left and right of an interface between two linear media.

Geometric Approximations of Electromagnetics

Consider a wave incident on the xy plane from the left, and the xy plane separates two linear media that supports wave propagation. Taking the propagation direction of the incident wave in the $+z$ direction, and polarized in the $+x$ direction

$$\tilde{\mathbf{E}_I}(z,t) = \tilde{E_{oI}} e^{i(k_1 z - \omega t)} \hat{\mathbf{x}} \tag{62}$$

$$\tilde{\mathbf{B}_I}(z,t) = \frac{1}{v_1} \tilde{E}_{oI} e^{i(k_1 z - \omega t)} \hat{\mathbf{y}} \tag{63}$$

after the wave interacts with the interface, a reflected wave is produced which travels to the right

$$\tilde{\mathbf{E}_R}(z,t) = \tilde{E_{oR}} e^{i(-k_1 z - \omega t)} \hat{\mathbf{x}} \tag{64}$$

$$\tilde{\mathbf{B}_R}(z,t) = \frac{1}{v_1} \tilde{E}_{oR} e^{i(-k_1 z - \omega t)} \hat{\mathbf{y}} \tag{65}$$

and a transmitted wave is produced on the right side of the xy plane, traveling to the left

$$\tilde{\mathbf{E}_T}(z,t) = \tilde{E_{oT}} e^{i(k_2 z - \omega t)} \hat{\mathbf{x}} \tag{66}$$

$$\tilde{\mathbf{B}_T}(z,t) = \frac{1}{v_1}\tilde{E}_{oT}e^{i(k_2 z-\omega t)}\hat{\mathbf{y}}. \tag{67}$$

In general, electromagnetic waves are incident at a surface at many different angles. For a monochromatic plane wave

$$\tilde{\mathbf{E}}_I(\mathbf{r},t) = \tilde{\mathbf{E}_{oI}}e^{i(\mathbf{k}_I\cdot\mathbf{r}-\omega t)},\ \tilde{\mathbf{B}}_I(\mathbf{r},t) = \frac{1}{v_1}(\hat{\mathbf{k}}_I\times\tilde{\mathbf{E}}_I) \tag{68}$$

are the incident electric and magnetic fields approaching from the left. After interacting with the interface, a reflected wave is produced

$$\tilde{\mathbf{E}}_R(\mathbf{r},t) = \tilde{\mathbf{E}_{oR}}e^{i(\mathbf{k}_R\cdot\mathbf{r}-\omega t)},\ \tilde{\mathbf{B}}_R(\mathbf{r},t) = \frac{1}{v_1}(\hat{\mathbf{k}}_R\times\tilde{\mathbf{E}}_R) \tag{69}$$

and a transmitted wave is produced

$$\tilde{\mathbf{E}}_T(\mathbf{r},t) = \tilde{\mathbf{E}_{oT}}e^{i(\mathbf{k}_T\cdot\mathbf{r}-\omega t)},\ \tilde{\mathbf{B}}_T(\mathbf{r},t) = \frac{1}{v_1}(\hat{\mathbf{k}}_T\times\tilde{\mathbf{E}}_T). \tag{70}$$

The frequency ω is the same for all three waves, and from the definition of angular frequency $\omega = kv$

$$k_I v_1 = k_R v_1 = k_T v_2 = \omega, \text{ or } \ k_I = k_R = \frac{v_2}{v_1}k_T = \frac{n_1}{n_2}k_T. \tag{71}$$

The combined fields $\tilde{\mathbf{E}}_I+\tilde{\mathbf{E}}_R$ and $\tilde{\mathbf{B}}_I+\tilde{\mathbf{B}}_R$ in medium 1 must be joined with the transmitted fields $\tilde{\mathbf{E}}_T$ and $\tilde{\mathbf{B}}_T$ using the boundary conditions. The fields share the mathematical form

$$(\ )e^{i(\mathbf{k}_I\cdot\mathbf{r}-\omega t)} + (\ )e^{i(\mathbf{k}_R\cdot\mathbf{r}-\omega t)} = (\ )e^{i(\mathbf{k}_T\cdot\mathbf{r}-\omega t)}, \text{ at } z = 0. \tag{72}$$

Since the boundary conditions must hold for all points on the plane, for all times, then the exponential factors must be equal. The spatial terms are then

$$\mathbf{k}_I\cdot\mathbf{r} = \mathbf{k}_R\cdot\mathbf{r} = \mathbf{k}_T\cdot\mathbf{r}, \text{ when } z = 0,. \tag{73}$$

or

$$x(k_I)_x + y(k_I)_y = x(k_R)_x + y(k_R)_y = x(k_T)_x + y(k_T)_y, \tag{74}$$

for all x and all y. Equation(74) can only hold if the components are separately equal. If $x = 0$, we have

$$(k_I)_y = (k_R)_y = (k_T)_y, \tag{75}$$

and if $y = 0$

$$(k_I)_x = (k_R)_x = (k_T)_x. \tag{76}$$

If we orient our axes so that $\mathbf{k}_I$ lies in the xz plane ($(k_I)_y = 0$), then $\mathbf{k}_R$ and $\mathbf{k}_T$ also lie in the xz plane. We can then generalize to conclude

- The plane which contains the incident, reflected, and transmitted waves, and the normal to the surface is called the **plane of incidence**.

Equation (76) implies that

$$k_I \sin\theta_I = k_R \sin\theta_R = k_T \sin\theta_T, \tag{77}$$

where θ_I is the **angle of incidence**, θ_R is the **angle of reflection**, and θ_T is the angle of transmission, or the **angle of refraction**. All of these angles are measured with respect to the normal. We can then generalize and state two laws. The first is the **law of reflection**

- The angle of incidence and angle of reflection are equal.

The second is the **law of refraction**, also known as **Snell's Law**

$$n_1 \sin\theta_I = n_2 \sin\theta_T \tag{78}$$

which gives us the angle of the transmitted angle with respect to the normal of the interface. These two laws, along with the definition of the plane of incidence, are the three fundamental laws of geometric optics. Any other waves, such as water waves or sound waves, will obey the same "optical" laws when they pass from one medium to anther.

Total Internal Reflection

Solving Snell's Law for θ_T

$$\sin\theta_T = \frac{n_1}{n_2} \sin\theta_I \tag{79}$$

This implies that if $n_1 < n_2$ then $\theta_T < \theta_I$ and if $n_1 > n_2$ then $\theta_T > \theta_I$. This implies that in the case of $n_1 > n_2$ for a certain angle of incidence $\theta_I = \theta_{critical}$, the refraction angle θ_T is 90°, and the light will stay confined in the material with higher index of refraction. From these assumptions, we have

$$\sin\theta_c = \frac{n_2}{n_1}\sin\theta_T = \frac{n_2}{n_1} \tag{80}$$

and the *critical angle* is therefore

$$\theta_c = \arcsin\frac{n_2}{n_1}. \tag{81}$$

A waveguide is a light confining device with a higher index of refraction in its core, and a lower index of refraction in its cladding. Light can be coupled into optical waveguides at angles at which total internal reflection happens inside of the waveguide.

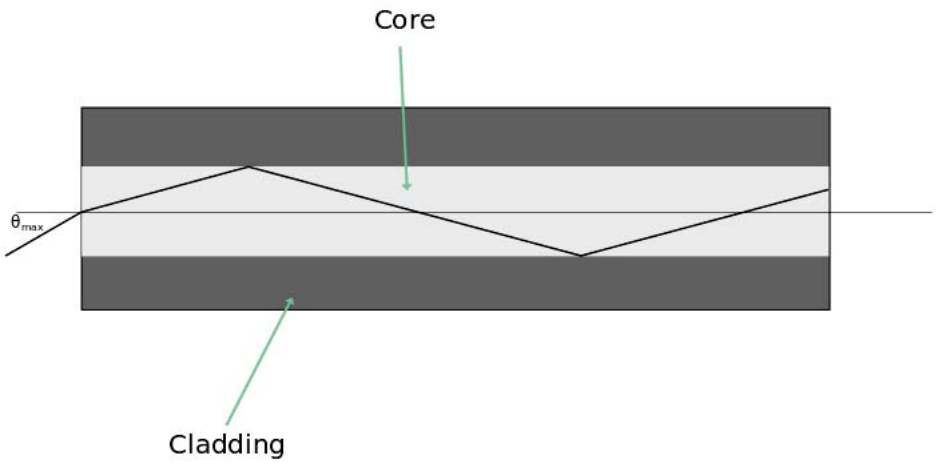

Figure 1: Total internal reflection inside a planar waveguide.

To find the maximum angle (relative to the normal of the waveguide) where we can still couple light into the waveguide, we use the $n = 1$ for air, and the *critical angle* derived above. From Snell's law, using the entrance plane of the waveguide as our interface, and $n = 1$ for air, we have

$$1 \cdot \sin\theta_{max} = n_1 \sin\left(\frac{\pi}{2} - \theta_c\right) = n_1\cos\theta_c \tag{82}$$

using this with the critical angle, we have

$$\sin\theta_{max} = n_1 \cos\theta_c = n_1\sqrt{1-\sin^2\theta_c} = n_1\sqrt{1-\left(\frac{n_2}{n_1}\right)^2}$$

$$\sin\theta_{max} = \sqrt{n_1^2 - n_2^2}. \tag{83}$$

The maximum angle also defines the *numerical aperture* (NA) of the waveguide

$$NA = \sqrt{n_1^2 - n_2^2}. \tag{84}$$

The Eikonal Equation

All propagation laws for pencils of rays of light can be derived from the *Eikonal Equation*. The equation gets its name from the Greek word $\epsilon\iota\kappa\tilde{\omega}\upsilon$ meaning image. Rays are the normals to light wavefronts, and also represent the direction of energy propagation of these waves. The Eikonal equation is a non-linear partial differential equation that can be derived from the scalar wave equation, using a first-order, plane wave-like solution of the time-harmonic electric and magnetic fields.

The scalar wave equation describes light propagation in a optical medium where the index of refraction varies slowly as a function of position. Using $v = \frac{1}{\sqrt{\mu\epsilon}} = \frac{c_0}{n}$, the scalar wave equation (57) becomes

$$\nabla^2\psi - \frac{n^2(x)}{c_0^2}\frac{\partial^2\psi}{\partial t^2} = 0 \tag{85}$$

where c_0 is the vacuum speed of light. A solution to (85) is of the form of a monochromatic wave

$$\psi = \phi(x)e^{-i\omega t} \tag{86}$$

and after taking the appropriate derivatives, the scalar wave equation becomes

$$\nabla^2\phi + k_0^2 n^2(x)\phi = 0 \tag{87}$$

where $k_0 \equiv \omega/c_0$ is the vacuum wavenumber, with units $1/length$. The solution to (87),

also known as the Helmholtz equation, is of the form

$$\phi(x) = A(x)e^{ik_0 S(x)} \tag{88}$$

where $S(x)$ is the eikonal function. Taking the appropriate derivatives of (88)

$$\nabla\phi = \{\nabla A + A(ik_0\nabla S)\}\, e^{ik_0 S(x)}$$

$$\nabla^2\phi = \left\{\nabla^2 A + \nabla A(ik_0\nabla S) + \nabla A(ik_0\nabla S) + A(ik_0\nabla^2 S) - Ak_0^2\left|\nabla S\right|^2\right\} e^{ik_0 S(x)}$$

$$\frac{\partial\psi}{\partial t} = A(-i\omega)e^{ik_0 S(x)}$$

$$\frac{\partial^2\psi}{\partial t^2} = -A\omega^2 e^{ik_0 S(x)}.$$

the Helmholtz equation becomes

$$\left\{\nabla^2 A + \nabla A ik_0\nabla S + \nabla A ik_0\nabla S + A ik_0\nabla^2 S - Ak_0^2\left|\nabla S\right|^2 - \frac{n^2(x)}{c_0^2}(-A\omega^2)\right\} e^{ik_0 S(x)} = 0$$

$$\left\{\nabla^2 A + \nabla A ik_0\nabla S + \nabla A ik_0\nabla S + A ik_0\nabla^2 S - Ak_0^2\left|\nabla S\right|^2 + k_0^2 n^2(x)A\right\} e^{ik_0 S(x)} = 0. \tag{89}$$

Looking at just the real part

$$\nabla^2 A - Ak_0^2\left|\nabla S\right|^2 + k_0^2 n^2(x)A = 0. \tag{90}$$

Dividing by $k_0^2 A$, and in the geometric limit $\frac{\nabla^2 A}{k_0^2 A} \to 0$ [3] [2], we have

$$\left|\nabla S(x)\right|^2 = n^2(x) \tag{91}$$

which is the eikonal equation.

We can define a local wave vector as

$$\vec{k} \equiv k_0\nabla S \tag{92}$$

and when $S(x) = \textit{constant}$ are surfaces of constant phase. Thus $\vec{k}$ points in the direction

normal to the constant phase surfaces. The eikonal equation implies that the magnitude of $\vec{k}$ is determined by the local index of refraction

$$k^2 = k_0^2 n^2(x). \tag{93}$$

The Vector Ray Equation

The vector ray equation is a vectorial equation that can determine ray paths in optical media. It will first be derived here from the eikonal equation, then from least action principles.

From The Eikonal Equation

The eikonal equation is the basic equation that describes light ray propagation in the geometric limit. It will be seen here that the eikonal equation can be further simplified to obtain the vector ray equation. Taking the square root of (91), and defining s as the arc-length of the ray, we have

$$\nabla S = n\frac{d\vec{\mathrm{r}}}{ds}. \tag{94}$$

Differentiating both sides of (94)

$$\frac{d}{ds}\left(\nabla S\right) = \frac{d}{ds}\left(n\frac{d}{ds}\right) \tag{95}$$

and using the definition of the grad operator ∇, we have

$$\frac{d\vec{r}}{ds}\cdot\nabla\left(\nabla S\right) = \frac{d}{ds}\left(n\frac{d\vec{r}}{ds}\right)$$

$$\frac{1}{n}\nabla S\cdot\nabla\left(\nabla S\right)) = \frac{d}{ds}\left(n\frac{d\vec{r}}{ds}\right)$$

$$\frac{1}{2n}\nabla[(\nabla S)^2] = \frac{d}{ds}\left(n\frac{d\vec{r}}{ds}\right)$$

$$\frac{1}{2n}\nabla n^2 = \frac{d}{ds}\left(n\frac{d\vec{r}}{ds}\right)$$

$$\nabla n = \frac{d}{ds}\left(n\frac{d\vec{r}}{ds}\right) \tag{96}$$

Equation (96) is the eikonal equation for ray vectors, or the *paraxial ray equation* whose solutions correspond to ray paths.

From Least Action Principles

Fermat's principle of least time states that a ray path between two specified points is traversed in the least amount of time required

$$\int_{x_1}^{x_2} nds = minimum \tag{97}$$

where n is the index of refraction, and ds is the ray path's arc length.

Hamilton's principle of least action is the broadest of all dynamical principles, and it yields the equations of motion for a classical particle

$$\int L\left(q_\alpha, \dot{q}_\alpha, t\right) dt = 0 \tag{98}$$

where L is the Lagrangian function equal to $T - V$ (kinetic minus potential energy), and is represented in generalized coordinates. Hamilton's principle states that the evolution of a dynamical system within a specified time interval is a stationary point of the action functional. Hamilton's principle minimizes functions of time, whereas Fermat's principle minimizes functions of length. From Hamilton's principle we can derive Lagrange's equations

$$\frac{d}{dt}\left(\frac{\partial L}{\partial \dot{q}}\right) = \frac{\partial L}{\partial q} \tag{99}$$

which yield the equations of motion for a particle in any system, given a known Lagrangian function. Lagrange's equations are the basic relationship between Hamiltonian and Newtonian mechanics.

From Fermat's principle, the *optical Lagrangian* can be determined, and then applied to Lagrange's equations to obtain the ray equations. Fermat's principle can then be written as

$$\delta \int n(x, y, z)\left(1 + \dot{x}^2 + \dot{y}^2\right)^{1/2} dz = 0 \tag{100}$$

where

$$L = L_{optical} = n(x, y, z)\left(1 + \dot{x}^2 + \dot{y}^2\right)^{1/2} \tag{101}$$

is the optical Lagrangian. If we choose the z-direction as the direction along which rays propagate, then z plays the same role as time in Hamiltonian mechanics. Lagrange's equations then become

$$\frac{d}{dz}\left(\frac{\partial L}{\partial \dot{x}}\right) = \frac{\partial L}{\partial x} \tag{102}$$

$$\frac{d}{dz}\left(\frac{\partial L}{\partial \dot{y}}\right) = \frac{\partial L}{\partial y} \tag{103}$$

From these two equations, we can derive the ray equation in vector form

$$\frac{d}{ds} n \frac{d\vec{r}}{ds} = \nabla n \tag{104}$$

which is the same result of (96), the vector ray equation.

CHAPTER III

THE HAMILTONIAN FORMULATION OF GEOMETRIC OPTICS

Here the Hamiltonian formulation of geometric optics is presented, and applied to our 2D quadratic index waveguide system. Recall that we are defining rays as the direction of energy propagation of the electromagnetic wavefronts. In an infinitesimal time dt, a point on the ray path moves a distance cdt in the direction of the unit vector $\vec{k}/k$. For the x component of the ray path

$$\frac{dx}{dt} = c(x)\frac{k_x}{k_0}. \tag{105}$$

Since the medium is continuously varying with position in the x direction

$$c(x) = \frac{c_0}{n(x)}. \tag{106}$$

and substituting (106) and (93) into (105)

$$\frac{dx}{dt} = \frac{c_0}{n^2(x)}\frac{k_x}{k_0} \tag{107}$$

From (92), $\vec{k} = \vec{k}(x(t))$, and the equation for the x component of $\vec{k}$ is

$$\frac{dk}{dt} = \frac{\partial k}{dx}\frac{dx}{dt}. \tag{108}$$

Since $\vec{k}$ is proportional to the gradient of the eikonal function (92),

$$\frac{\partial k_x}{\partial x} = \frac{\partial k}{\partial x} \tag{109}$$

and substituting (105) yields

$$\frac{dk_x}{dt} = \frac{c_0}{k_0}\frac{1}{n^2(x)}\frac{1}{2}\frac{\partial k^2}{dx} \tag{110}$$

and from (93)

$$\frac{dk_x}{dt} = c_0 k_0 \frac{1}{n(x)}\frac{\partial n(x)}{\partial x}. \tag{111}$$

By noting that $\omega = c(x)k = \frac{c_0}{n(x)}k$, we can obtain a correspondence with Hamiltonian

mechanics. From (105) and (111)

$$\frac{dx}{dt} = \frac{\partial \omega}{\partial k_x} \tag{112}$$

$$\frac{dk_x}{dt} = -\frac{\partial \omega}{\partial x} \tag{113}$$

which represent Hamilton's equations for particle dynamics.

For ray propagation in a waveguide, we assume that the ray never turns back upon itself, and taking z as the optical axis

$$\frac{dx}{dz} \neq 0. \tag{114}$$

This allows us to describe the ray paths by the one-way equations. Dividing equation (107) by dz/dt, we have

$$\frac{dx}{dt}\frac{dt}{dz} = \frac{c_0}{n^2(x)}\frac{k_x}{k_0}\frac{dt}{dz}. \tag{115}$$

The ray path in the z direction is

$$\frac{dz}{dt} = c(x)\frac{k_z}{k_0} \tag{116}$$

and after solving for k_z, (115) becomes

$$\frac{dx}{dz} = \frac{k_x}{k_z}. \tag{117}$$

Dividing (111) by dz/dt

$$\frac{dk_x}{dt}\frac{dt}{dz} = c_0 k_0 \frac{1}{n(x)}\frac{\partial n(x)}{\partial x}\frac{dt}{dz} \tag{118}$$

$$\frac{dk_x}{dz} = \frac{k_0^2}{k_z} n \frac{\partial n(x)}{\partial x} \tag{119}$$

If we define $p \equiv k_x/k_0$ as the new conjugate variable to x, the dynamical system for the ray trajectory becomes

$$\frac{dx}{dz} = \frac{p}{\sqrt{n^2 - p^2}} \tag{120}$$

$$\frac{dp}{dz} = \frac{n\frac{\partial n}{\partial x}}{\sqrt{n^2 - p^2}}. \tag{121}$$

The equations for this dynamical system can be rewritten in the form of Hamilton's equations

$$\frac{dx}{dz} = \frac{\partial H}{\partial p} \tag{122}$$

$$\frac{dp}{dz} = -\frac{\partial H}{\partial x} \tag{123}$$

where the Hamiltonian is given by

$$H = -\sqrt{n^2(x,y) - p^2}. \tag{124}$$

The angle between the ray and the optical axis z is given by

$$\tan\theta = \frac{dx}{dz}. \tag{125}$$

In terms of the index of refraction n and the ray angle θ, the Hamiltonian and momentum can be written as

$$H = -n\cos\theta \tag{126}$$

$$p = n\sin\theta. \tag{127}$$

If the index of refraction is independent of the axial coordinate, then the Hamiltonian $H = -n\cos\theta$ is a constant along the ray path. This is a generalization of Snell's Law for a medium with continuously varying index of refraction in transverse x-direction. The presence of cosine rather than sine is due to the definition of the angle θ relative to the optical axis.

Derivation of Ray Trajectories in Quadratic Index Profile Waveguides

The most common index profile for gradient-index optical waveguides is a quadratic function of the transverse coordinate x. For a rectangular optical waveguide of fixed thickness a, the profile is

$$n^2(x) = n_0^2 - \left(n_0^2 - 1\right)\frac{x^2}{a^2} \tag{128}$$

for this index profile, the Hamiltonian is

$$H = -\sqrt{n^2(x) - p^2}. \tag{129}$$

Hamilton's equations (120) and (121) then become

$$\frac{dx}{dz} = \frac{p}{\sqrt{n^2 - p^2}} \tag{130}$$

$$\frac{dp}{dz} = \frac{-(n_o^2 - n_1^2)x}{a^2\sqrt{n^2 - p^2}}. \tag{131}$$

Using the chain rule

$$\frac{dp}{dx} = \frac{-(n_o^2 - n_1^2)x}{a^2 p}. \tag{132}$$

Separating variables, we have

$$pdp = \frac{-(n_o^2 - n_1^2)}{a^2} x dx \tag{133}$$

$$p^2 = p_o^2 + \frac{(n_o^2 - n_1^2)x_o^2}{a^2} - \frac{(n_o^2 - n_1^2)x^2}{a^2}. \tag{134}$$

We now define

$$N^2 \equiv p_o^2 + \frac{(n_o^2 - n_1^2)x_o^2}{a^2} \tag{135}$$

and

$$\Delta n^2 \equiv \frac{(n_o^2 - n_1^2)}{a^2}. \tag{136}$$

The momentum then becomes

$$p^2 = N^2 - \Delta n^2 x^2 \tag{137}$$

$$p = \sqrt{N^2 - \Delta n^2 x^2}. \tag{138}$$

Substitution of p and $n^2(x) = n_o^2 - \frac{(n_o^2 - n_1^2)x^2}{a^2} = n_o^2 - \Delta n^2 x^2$ into (130) gives

$$\frac{dx}{dz} = \frac{\sqrt{N^2 - \Delta n^2 x^2}}{\sqrt{n_o^2 - N^2}} \tag{139}$$

rearranging as

$$\frac{dx}{\sqrt{\left(\frac{N}{\Delta n}\right)^2 - x^2}} = \frac{\Delta n}{\sqrt{n_o^2 - N^2}} dz \tag{140}$$

then integrating gives

$$\arcsin\left(\frac{x}{\frac{N}{\Delta n}}\right) - \arcsin\left(\frac{x_o}{\frac{N}{\Delta n}}\right) = \left(\frac{\Delta n}{\sqrt{n_o^2 - N^2}}\right)(z - z_o) \tag{141}$$

$$x = \left(\frac{N}{\Delta n}\right) sin\left[\arcsin\left(\frac{x_o}{\frac{N}{\Delta n}}\right) + \left(\frac{\Delta n}{\sqrt{n_o^2 - N^2}}\right)(z - z_o)\right]. \tag{142}$$

Looking just at $N \equiv \sqrt{p_o^2 + (n_o^2 - n_1^2)\frac{x^2}{a^2}} = \sqrt{p_o^2 + \Delta n^2 x_o^2}$, and using $p = nsin\theta = \sqrt{n_o^2 - \Delta n^2 x^2} sin\theta$, we have after rearranging

$$N = \sqrt{n_o^2 sin^2\theta_o + cos^2\theta_o \Delta n^2 x_o^2}. \tag{143}$$

If the initial angle is $\theta_o = 0$ at $z_o = 0$, then $cos\theta_o = 1$ and $N = \sqrt{\Delta n^2 x_o^2}$ and $\frac{N}{\Delta n} = \frac{\sqrt{\Delta n^2 x_o^2}}{\Delta n} = x_o$, (142) becomes

$$x = x_o sin\left[\arcsin\left(\frac{x_o}{x_o}\right) + \left(\frac{\Delta n}{\sqrt{n_o^2 - \Delta n^2 x_o^2}}\right) z\right] \tag{144}$$

$$x = x_o sin\left[\frac{\pi}{2} + \left(\frac{\Delta n}{\sqrt{n_o^2 - \Delta n^2 x_o^2}}\right) z\right] \tag{145}$$

$$x = x_o cos\left[\left(\frac{\Delta n}{\sqrt{n_o^2 - \Delta n^2 x_o^2}}\right) z\right]. \tag{146}$$

From $k = 2\pi/\lambda$, we define

$$\lambda \equiv \frac{2\pi\sqrt{n_o^2 - \Delta n^2 x_o^2}}{\Delta n}, \tag{147}$$

then the general expression for ray trajectories is

$$x = x_o cos\left(\frac{2\pi z}{\lambda}\right) \tag{148}$$

CHAPTER IV

COMPUTATIONAL SIMULATIONS OF RAY BUNDLES IN QUADRATIC INDEX WAVEGUIDES

The analytic solution for ray trajectories in quadratic index waveguides (148) was simulated in Octave. First, refractive indices are defined to be $n_o = 4$ along the optical axis, and $n_1 = 1$ at the boundary. The characteristic lengthscale of the simulation (and all simulation in this thesis) is in microns. The waveguide half-width (distance to the boundary from the center of the waveguide) is 5 microns, and the waveguide length is 32 microns. The ray's initial positions on the left boundary were given equal spacings, and each with an initial angle of $\theta_0 = 0$ degrees. All of this information is passed into a function that calculates equation (147), and then equation (148). The result of this function is a column vector for each ray that gives the transverse position at all axial locations. Figure 2 is the plot from the simulation results (see Appendix A for code)

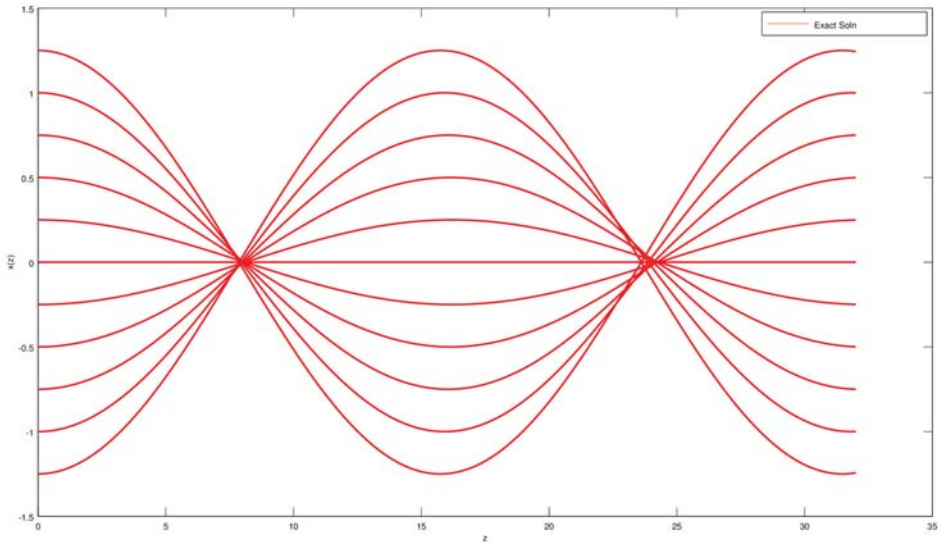

Figure 2: Ray bundle using general solution from Hamilton's Equations

Note that from Figure 2, we see the wavelength dependence on the initial position of the ray predicted in (147). This is more clearly seen at the second node. This is unique from the other systems with oscillatory solutions such as the classical harmonic oscillator.

Numerical Solutions To Hamilton's Equations

The problem of light propagation in quadratic index media involve solving differential equations for some initial values. The differential equations are Hamilton's equations, and the initial values that must be specified are the initial transverse positions of each ray, and the initial axial position, which in all of our simulations is at $z = 0$. Given these initial values, we can propagate Hamilton's equations forward as the axial position increases. Euler's method is a numerical technique to solving ordinary differential equations. Hamilton's equations (120) and (121) are of the form

$$\frac{dx}{dt} = f(x, t). \tag{149}$$

Taking the Taylor series expansion of x about t gives

$$x(t + \Delta t) = x(t) + \frac{dx}{dt}\Delta t + \frac{1}{2!}\frac{d^2x}{dt^2}(\Delta t)^2 + \cdots . \tag{150}$$

where $x(t)$ is the initial value of the function. If we take Δt to be small enough so that the terms second order and higher are negligible, then we can ignore those terms, and we are left with an approximation for the value of the function at time step $t + \Delta t$.

$$x(t + \Delta t) \approx x(t) + \frac{dx}{dt}\Delta t. \tag{151}$$

This approach is called the *Euler method*. Euler's method can be expressed by using the indices i

$$x(t_{i+1}) \approx x(t_i) + f(x(t_i), t_i)\Delta t \tag{152}$$

where $x(t_i)$ is the initial value of the function. The local order of the approximation is determined by the order in Δt to which the approximation agrees with the exact solution. Euler's method is a first order approximation at t_{i+1}.

For an improved approximation method, we can keep higher orders of the Taylor expansion. We can think of the problem of solving differential equations of the form of equation (149) as integrating dx/dt from t to $t+\Delta t$. Then, from the mean value theorem, there exists a value t_m in the interval where the exact solution is found while stopping at first order in

Δt

$$x(t+\Delta t) = x(t) + \frac{dx}{dt}|_{t_m}\Delta t. \tag{153}$$

The slope $dx/dt|_{t_m}$ contains information of the curvature (second and higher order terms). By properly estimating t_m and $dx/dt|_{t_m}$, approximations of higher order than the Euler method can be obtained. One of those approximations is the second-order Runge-Kutta approximation

$$x(t+\Delta t) = x(t) + f(x', t')\Delta t \tag{154}$$

where

$$x' = x(t) + \frac{1}{2}f(x(t), t)\Delta t \tag{155}$$

$$t' = t + \frac{1}{2}\Delta t. \tag{156}$$

The expression t' is the midpoint of the interval, and x' is the Euler approximated value of x at t', and this approximation is accurate to second order, and first order accurate globally. The Runge-Kutta approximation estimates the slope $dx/dt|_{t_m}$ by a weighted average of several terms of the form $f(x', t')$ where t'_i are suitably chosen values in the interval $[t, t + \Delta t]$, and x'_i are obtained by an *Euler-like* approximation. Anther popular higher order approximation is the fourth-order Runge-Kutta method

$$x(t+\Delta t) \equiv x(t) + \frac{1}{6}\left[f(x'_1, t'_1) + 2f(x'_2, t'_2) + 2f(x'_3, t'_3) + f(x'_4, t'_4)\right]\Delta t \tag{157}$$

where

$$x'_1 = x(t)$$

$$x'_2 = x(t) + \frac{1}{2}f(x'_1, t'_1)\Delta t$$

$$x'_3 = x(t) + \frac{1}{2}f(x'_2, t'_2)\Delta t$$

$$x'_4 = x(t) + f(x'_3, t'_3)\Delta t$$

and

$$t'_1 = t$$

$$t_2' = t + \frac{1}{2}\Delta t$$

$$t_3' = t + \frac{1}{2}\Delta t$$

$$t_4' = t + \Delta t.$$

This fourth-order Runge-Kutta method requires the calculation of $f(x', t')$ four times and Euler approximations four times, and thus requires roughly four times the computing requirements per step of the Euler method at the same accuracy. But we can chose larger values of Δt than with the Euler method at the same accuracy. This makes the fourth-order Runge-Kutta method the first choice for approximation methods for computational problems requiring high accuracies.

Matlab's `ode45` function can be used to solve Hamilton's equations. This function solves non-stiff differential equations. It is based on an explicit Runge-Kutta method. The syntax for using `ode45` is

```
[Z,X]=ode45(@funcname,t,x0,options,param)
```
(158)

where `Z` is a column vector of axial points on the waveguide, and `X` is the solution array for the transverse position of the ray at the respective axial position. For our simulation, `t` is the interval of integration over a defined axial region. The `ode45` solver will use the first element of this vector, and integrate from the first element to the last. A row in the solution array `X` contains two elements, which correspond to the solutions of Hamilton's equations for $x(z)$ and $p(z)$ at the corresponding axial location.

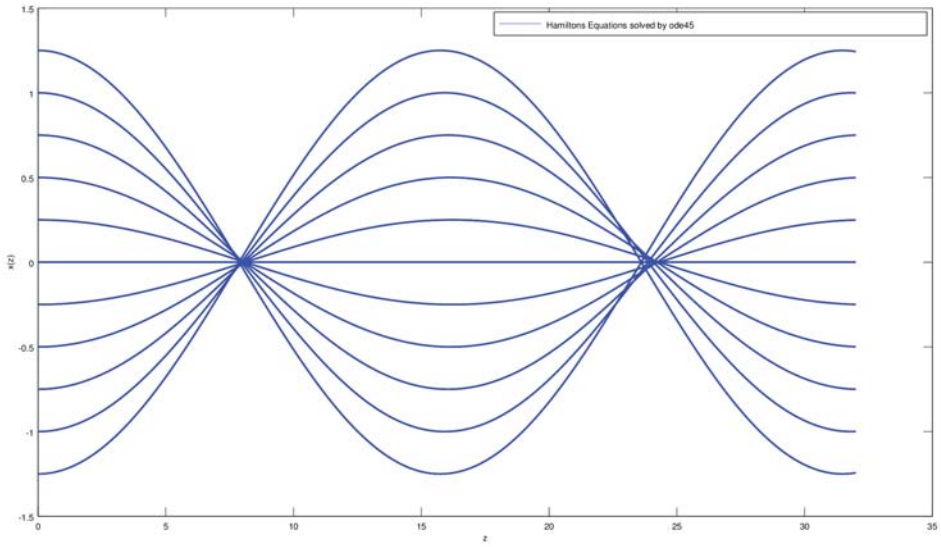

Figure 3: Ray bundle using ode45 to solve Hamilton's equations.

The initial condition `y0` is a row vector of two elements, the first being the initial position, and the second element is the initial momentum $p\,(z=0) = p_0 = n_0 \sin\theta_0$. The initial angle θ_0, indices's of refraction n_0 and n_1, and a_0, the maximum transverse distance from the center of the waveguide are all given.

A comparison of the two simulations can be made by overlaying the `ode45` plot over the analytic solution simulation. Figure 44 is the overlay plot of both simulations, and both are in exact agreement with each other.

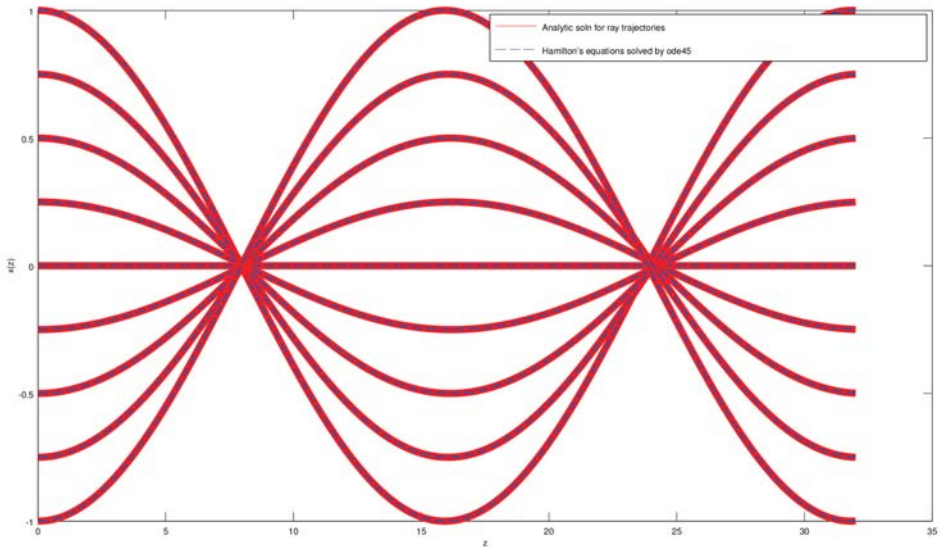

Figure 4: Comparisons of analytic solution, and ode45 solution of Hamilton's equations.

Simulation of a Gaussian Ray Bundle

In order to get insights of how a real laser beam will propagate in quadratic index waveguides from the ray trajectories presented, we have to create an initial ray distribution that represents a Gaussian function. To create a Gaussian ray bundle we define ray spacings that are proportional to a Gaussian function as

$$x_{i+1} = x_i + \alpha e^{x_i^2/2\sigma} \tag{159}$$

where α is the initial spacing from the on-axis ray to both of its adjacent rays on each side. The Gaussian ray spacing defined by (159) is implemented to the analytic solution for ray trajectories, and the result is seen in Figure 5.

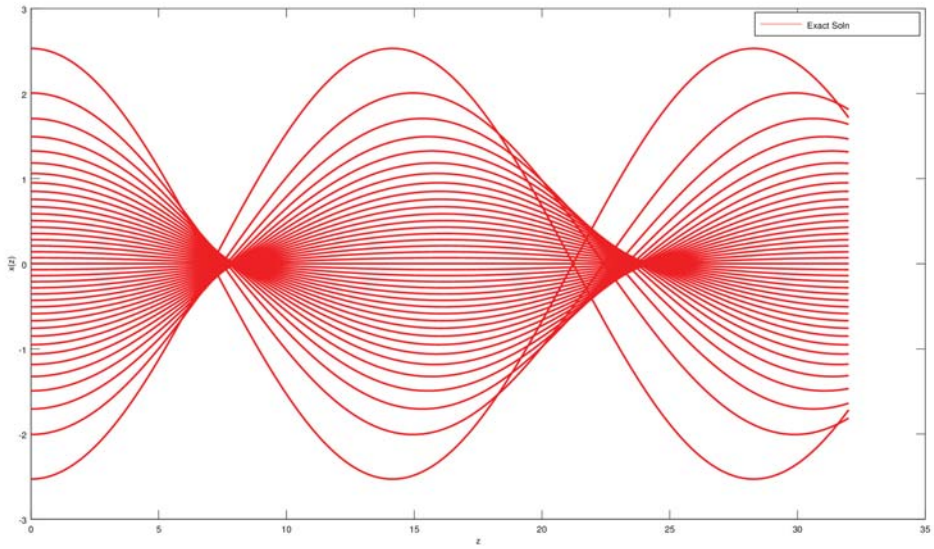

Figure 5: Gaussian Ray Bundle.

Again we see the wavelength dependence on the initial position of each ray, and we can predict that this will correspond to focusing regions of a real laser beam propagating in a quadratic index waveguide.

CHAPTER V

WAVE OPTICS TREATMENT OF LIGHT PROPAGATION IN QUADRATIC INDEX WAVEGUIDES

Derivation of Gaussian Beams and its Properties

Starting with the Helmholtz (scalar) wave equation (87), and taking $n(x) = 1$

$$\nabla^2\phi + k^2\phi = 0 \tag{160}$$

where ψ is the complex field amplitude for any polarization of the electric field, and $k = 2\pi/\lambda = \omega/v = \omega\sqrt{\epsilon\mu}$ is the vacuum wave number. Taking ϕ in the z direction as

$$\phi = u(x, y, z)e^{-ikz} \tag{161}$$

the derivatives are

$$\nabla\phi = \nabla u e^{-ikz} - iku e^{-ikz} \tag{162}$$

$$\nabla^2\phi = \nabla^2 u e^{-ikz} - 2ik\nabla u e^{-ikz} - k^2 u e^{-ikz} \tag{163}$$

and substituting back into the (160), we have

$$\left(\nabla^2 u - 2ik\nabla u\right) e^{-ikz} = 0. \tag{164}$$

At this point we impose the *paraxial approximation* in wave analysis. The first approximation is that the variation of propagation is slow on the scale of the wavelength λ. Mathematically this is expressed as

$$\left|\frac{\partial^2 u}{\partial z^2}\right| \ll 2k\left|\frac{\partial u}{\partial z}\right|. \tag{165}$$

The next approximation is that the variation of propagation is slow in the transverse direction

$$\left|\frac{\partial^2 u}{\partial z^2}\right| \ll \left|\frac{\partial^2 u}{\partial x^2}\right|, \left|\frac{\partial^2 u}{\partial y^2}\right|. \tag{166}$$

the Helmholtz equation (160) them becomes

$$\frac{\partial^2 u}{\partial x^2} + \frac{\partial^2 u}{\partial y^2} - 2ik\frac{\partial u}{\partial z} = 0. \tag{167}$$

Equation (167) is called the *paraxial wave equation.*

To solve the paraxial wave equation, we assume the trial solution has the form [11]

$$u = Aexp\left\{-i\left[P(z) + \frac{\pi r^2}{\lambda q(z)}\right]\right\} \tag{168}$$

where $r^2 = x^2 + y^2$. We can rewrite u using $k = 2\pi/\lambda$, and $A = 1$ [9], [11],

$$u = exp\left\{-i\left[P(z) + \frac{k(x^2+y^2)}{2q(z)}\right]\right\}. \tag{169}$$

Taking the appropriate derivatives

$$\frac{\partial u}{\partial x} = -\frac{ikx}{q(z)}u$$

$$\frac{\partial^2 u}{\partial x^2} = \left(-\frac{ikx}{q(z)}\right)\left(-\frac{ikx}{q(z)}\right)u - \frac{ik}{q(z)}u = -\frac{k^2x^2}{q^2(z)}u - \frac{ik}{q(z)}u$$

and similarly for $\partial^2 u/\partial y^2$

$$\frac{\partial^2 u}{\partial y^2} = -\frac{k^2y^2}{q^2(z)}u - \frac{ik}{q(z)}u$$

and

$$\frac{\partial u}{\partial z} = -i\left[P'(z) - \frac{kr^2}{q^2(z)}q'(z)\right]u$$

the Helmholtz equation then becomes

$$-\frac{k^2x^2}{q^2(z)} - \frac{ik}{q(z)} - \frac{k^2y^2}{q^2(z)} - i\frac{k}{q(z)} - 2ik\left[-iP'(z) + i\frac{kr^2}{2q^2(z)}q'(z)\right] = 0$$

$$-\frac{k^2r^2}{q^2(z)}(1 - q'(z)) - 2k\left(\frac{i}{q(z)} + P'(z)\right) = 0.$$

Each term must vanish independently, so

$$\frac{dq(z)}{dz} = 1 \tag{170}$$

and

$$\frac{dP(z)}{dz} = -\frac{i}{q(z)}. \tag{171}$$

The solution to (170) is $q(z) = q_o + z$.

Next we introduce the *complex beam parameter*, which relates two real beam parameters R and w [9]

$$\frac{1}{q} = \frac{1}{R} - i\frac{\lambda}{\pi w^2}. \tag{172}$$

When (172) is substituted into the trial solution (169), the physical meaning of the parameters R and w is seen. The parameter R is the radius of curvature of the wavefront at z, and w is the beam radius, which is defined as the distance from the maximum amplitude of the field, to the point where it decreases to the value $1/e$. The *spot size* of the beam is $2w$, and is also called the *beam diameter*. The minimum diameter of the beam is $2w_0$, and is called the *beam waist*. The complex beam parameter at the waist is purely imaginary [9]

$$q_0 = i\frac{\pi w_0^2}{\lambda}. \tag{173}$$

so that the solution to (170) then becomes

$$q = i\frac{\pi w_0^2}{\lambda} + z. \tag{174}$$

Substituting (174) into (172), we have

$$\frac{1}{i\frac{\pi w_0^2}{\lambda} + z} = \frac{1}{R} - i\frac{\lambda}{\pi w^2}$$

$$\frac{-i\frac{\pi w_0^2}{\lambda} + z}{\frac{\pi^2 w_0^4}{\lambda^2} + z^2} = \frac{1}{R} - i\frac{\lambda}{\pi w^2}$$

$$-i\frac{\pi w_0^2}{\lambda} + z = \frac{1}{R}\left(\frac{\pi^2 w_0^4}{\lambda^2} + z^2\right) - i\frac{\lambda}{\pi w^2}\left(\frac{\pi^2 w_0^4}{\lambda^2} + z^2\right) \tag{175}$$

Equating the imaginary parts of (175), we obtain the expression for the square of the beam radius

$$-i\frac{\pi w_0^2}{\lambda} = -i\frac{\lambda}{\pi w^2}\left(\frac{\pi^2 w_0^4}{\lambda^2} + z^2\right)$$

$$w^2(z) = \frac{\lambda^2}{\pi^2 w_0^2}\left(\frac{\pi^2 w_0^4}{\lambda^2} + z^2\right)$$

$$w^2(z) = w_0^2\left[1 + \left(\frac{\lambda z}{\pi w_0^2}\right)^2\right]. \tag{176}$$

Equating the real parts of (175), we obtain the expression for the radius of curvature

$$z = \frac{1}{R}\left(\frac{\pi^2 w_0^4}{\lambda^2} + z^2\right)$$

$$R(z) = \frac{1}{z}\left(\frac{\pi^2 w_0^4}{\lambda^2} + z^2\right)$$

$$R(z) = z\left[\left(\frac{\pi w_0^2}{\lambda z}\right)^2 + 1\right]. \tag{177}$$

The beam contour of $w(z)$ is a hyperbola, with asymptotes that make an angle with the optical axis z

$$\theta = \frac{\lambda}{\pi w_0}. \tag{178}$$

Dividing (177) by (176), we obtain the relation

$$\frac{\lambda z}{\pi w_0^2} = \frac{\pi w^2}{\lambda R} \tag{179}$$

which can be used to express w_0 and z in terms of w and R

$$w_0^2 = \frac{w^2}{\left[\left(\frac{\pi w^2}{\lambda R}\right)^2 + 1\right]} \tag{180}$$

$$z = \frac{R}{\left[\left(\frac{\lambda R}{\pi w^2}\right) + 1\right]}. \tag{181}$$

Next we solve the differential equation for $P(z)$, equation (171)

$$\frac{dP(z)}{dz} = -\frac{i}{q(z)} = -\frac{i}{i\frac{\pi w_0^2}{\lambda} + z} \tag{182}$$

and integrating (182) yields

$$iP(z) = \ln\left[1 - i\left(\frac{\lambda z}{\pi w_0^2}\right)\right]$$

$$iP(z) = \ln\sqrt{1 + \left(\frac{\lambda z}{\pi w_0^2}\right)^2} - i\tan^{-1}\left(\frac{\lambda z}{\pi w_0^2}\right). \tag{183}$$

The real part of $P(z)$ is the phase shift difference between the Gaussian beam and an ideal plane wave. The imaginary part represents the expected intensity decrease of the beam due to the expansion of the beam. The trial solution (161) of the Helmholtz wave equation is now

$$\phi = \frac{w_0}{w}\exp\left\{-i(kz - \Phi) - r^2\left(\frac{1}{w^2} + \frac{ik}{2R}\right)\right\} \tag{184}$$

where $\Phi = \tan^{-1}\left(\lambda z/\pi w_0^2\right)$.

Hermite Polynomials

In Cartesian coordinates, the paraxial wave equation can be satisfied by

$$u(x,y,z) = g\left(\frac{x}{w}\right)\cdot h\left(\frac{y}{w}\right)\cdot\exp\left\{-i\left[P + \frac{k}{2q}(x^2+y^2)\right]\right\} \tag{185}$$

were g is a function of x and z, and h is a function of y and z. Looking at only the transverse dimension x, (185) is

$$u(x,z) = g\left(\frac{x}{w}\right)\cdot\exp\left\{-i\left[P + \frac{kx^2}{2q}\right]\right\} \tag{186}$$

Using (186) in the paraxial wave equation (167), we obtain Hermite's differential equation for the function g

$$\frac{d^2H_n}{dx^2} - 2x\frac{dH_n}{dx} + 2nH_n = 0. \tag{187}$$

where H_n are the solutions to (187,) are the Hermite polynomials where n defines its order.

The Hermite polynomials are a complete set of orthogonal functions in the interval

$[-\infty, \infty]$, and have the orthogonality relation

$$\int_{-\infty}^{\infty} dx e^{-x^2} H_n(x) H_m(x) = 2^n n! \sqrt{\pi} \delta_{nm}. \tag{188}$$

This relation can be used to define a set of polynomials $\gamma_n(x)$

$$\gamma_n(x) = \frac{1}{\sqrt{2^n n! \sqrt{\pi}}} e^{-\frac{x^2}{2}} H_n(x), \ n = 0, 1, 2, ... \tag{189}$$

so that the orthogonality relation becomes

$$\int_{-\infty}^{\infty} dx \gamma_n(x) \gamma_m(x) = \delta_{nm}. \tag{190}$$

Since this defines a complete set, then any well-behaved function in the interval $[-\infty, \infty]$ can be expanded in terms of $\gamma_n(x)$

$$f(x) = \sum_{n=0}^{\infty} C_n \gamma_n(x) \tag{191}$$

where the coefficients can be found by

$$C_n = \int_{-\infty}^{\infty} dx' f(x') \gamma_n(x') = (\text{constant} \neq 0). \tag{192}$$

Hermite Polynomial Expansion of Gaussian Beams

A Gaussian function is defined as

$$f(x) = e^{-\frac{x^2}{2\sigma^2}} = e^{-\frac{b^2}{2\sigma^2}\left(\frac{x^2}{b^2}\right)} = e^{-\frac{b^2}{2\sigma^2} x'^2} \tag{193}$$

which we can expand in terms of Hermite polynomials ([4] equation 4.51) on the left boundary $z = 0$ as

$$f(x) = \sum_{n=0}^{\infty} C_n \gamma_n(x). \tag{194}$$

Using (192), the expansion (194) becomes

$$f(x) = \sum_{n=0}^{\infty} \int_{-\infty}^{\infty} dx' f(x') \gamma_n(x') \gamma_n(x) \tag{195}$$

and then substituting (189), we have

$$f(x) = \sum_{n=0}^{\infty} \left[\int_{-\infty}^{\infty} dx' \frac{f(x')}{\sqrt{2^n n! \sqrt{\pi}}} e^{-\frac{x'^2}{2}} H_n(x') \right] \frac{1}{\sqrt{2^n n! \sqrt{\pi}}} e^{\frac{-x^2}{2}} H_n(x) \tag{196}$$

$$f(x) = \sum_{n=0}^{\infty} \frac{1}{2^n n! \sqrt{\pi}} \left[\int_{-\infty}^{\infty} dx' f(x') e^{-\frac{x'^2}{2}} H_n(x') \right] e^{\frac{-x^2}{2}} H_n(x) \tag{197}$$

Just looking at the integral in the square bracket

$$\int_{-\infty}^{\infty} dx' f(x') e^{-\frac{b^2 x^2}{2\sigma^2}} e^{-\frac{x'^2}{2}} H_n(x') = \int_{-\infty}^{\infty} dx' e^{-\frac{1}{2}\left(\frac{b^2}{\sigma^2}+1\right)x^2} H_n(x'). \tag{198}$$

Since we are modeling a Gaussian beam, which by symmetry is an even function, we only use the even orders of the Hermite polynomials, $n = 2m$. Using the substitution $\rho^2 = \left(-\frac{1}{2}\left(\frac{b^2}{\sigma^2}+1\right)\right)$ for the exponential on the right side of (198), and using the result from Bayin [4] problem 4.10, (198) becomes

$$\int_{-\infty}^{\infty} dx' f(x') e^{-\frac{b^2 x^2}{2\sigma^2}} e^{-\frac{x'^2}{2}} H_n(x') = \frac{(2m)!}{m!} \frac{\sqrt{\pi}}{\rho} \left(\frac{1-\rho^2}{\rho^2} \right)^m. \tag{199}$$

The expansion of the Gaussian function is now

$$f(x) = \sum_{n=0}^{\infty} \frac{1}{2^{2m}(2m)!\sqrt{\pi}} \frac{(2m)!}{m!} \frac{\sqrt{\pi}}{\rho} \left(\frac{1-\rho^2}{\rho^2} \right)^m e^{-\frac{x^2}{2}} H_{2m}(x) \tag{200}$$

$$f(x) = \sum_{n=0}^{\infty} \frac{1}{4^m m!} \frac{1}{\rho} \left(\frac{1-\rho^2}{\rho^2} \right)^m e^{-\frac{x^2}{2}} H_{2m}(x) \tag{201}$$

Derivation of Analytic Solutions for Field Intensities in Quadratic Index Waveguides

The analytic solution for modes in a planar quadratic index waveguide is derived here from the reduced scalar wave equation, or the Helmholtz equation

$$\nabla^2\phi + n^2(x)k_0^2 = 0 \tag{202}$$

where $n^2(x)$ is defined by (1), and $k_0 = 2\pi/\lambda$ is the vacuum wave number. Waves are assumed to have a harmonic time dependence $e^{i\omega t}$. The Helmholtz equation (202) is solved using the trial solution

$$\phi = f(x)e^{-i\beta z} \tag{203}$$

where we are only considering one transverse dimension x. A solution of the form (203) is a mode of the quadratic index waveguide, and the functions f and β are undetermined at this point. Taking the appropriate derivatives of (203)

$$\frac{\partial\phi}{\partial z} = -f(i\beta)e^{-i\beta z}$$

$$\frac{\partial^2\phi}{\partial z^2} = -f\beta^2 e^{-i\beta z}$$

and the substituting these derivative and the index of refraction (1) into (202), we have

$$\frac{d^2f}{dx^2} + (n_o^2k_o^2 - \beta^2 - k_o^2(n_o^2 - n_1^2)\frac{x^2}{a_o^2})f = 0. \tag{204}$$

$$f''(x)e^{-i\beta z} - \beta^2 f(x)e^{i\beta z} + k_0^2\left(n_0^2 - \left(n_0^2 - n_1^2\right)\frac{x^2}{a_0^2}\right)f(x)e^{-i\beta z} = 0. \tag{205}$$

The exponential terms vanish, and we have

$$f''(x) - \beta^2 f(x) + k_0^2\left(n_0^2 - \left(n_0^2 - n_1^2\right)\frac{x^2}{a_0^2}\right)f(x) = 0 \tag{206}$$

This equation can be transformed into the form of the quantum harmonic oscillator (Ap-

pendix F) by making the following substitution

$$\xi = \sqrt{k_o}\left(\frac{n_0^2 - n_1^2}{a_0^2}\right)^{1/4} x. \tag{207}$$

Solving (207) for x

$$x = \frac{\xi}{\sqrt{k_o}\left(\frac{n_0^2-n_1^2}{a_0^2}\right)^{1/4}}. \tag{208}$$

Using the chain rule

$$\frac{df}{dx} = \frac{df}{d\xi}\frac{d\xi}{dx} \tag{209}$$

we have

$$\frac{df}{dx} = \frac{df}{d\xi}\sqrt{k_o}\left(\frac{n_0^2 - n_1^2}{a_0^2}\right)^{1/4}$$

$$\frac{d^2f}{dx^2} = \frac{d}{d\xi}\left[\frac{df}{d\xi}\sqrt{k_o}\left(\frac{n_0^2 - n_1^2}{a_0^2}\right)^{1/4}\right]\frac{d\xi}{dx}$$

$$\frac{d^2f}{dx^2} = \frac{d^2f}{d\xi^2}k_0\left(\frac{n_0^2 - n_1^2}{a_0^2}\right)^{1/2} \tag{210}$$

Equation (206) becomes

$$\frac{d^2f}{d\xi^2}k_0\left(\frac{n_0^2 - n_1^2}{a_0^2}\right)^{1/2} + \left(n_0^2k_0^2 - \beta^2\right)f(\xi) - k_0^2\left(\frac{n_0^2 - n_1^2}{a_0^2}\right)\frac{\xi^2}{k_0\left(\frac{n_0^2-n_1^2}{a_0^2}\right)^{1/2}}f(\xi) = 0 \tag{211}$$

$$\frac{d^2f}{d\xi^2} + \frac{n_0^2k_0^2 - \beta^2}{k_0\left(\frac{n_0^2-n_1^2}{a_0^2}\right)^{1/2}}f(\xi) - \frac{k_0\left(\frac{n_0^2-n_1^2}{a_0^2}\right)^{1/2}}{k_0\left(\frac{n_0^2-n_1^2}{a_0^2}\right)^{1/2}}\xi^2 f(\xi) = 0. \tag{212}$$

Defining

$$\sigma = \frac{n_0^2k_0^2 - \beta^2}{k_0\left(\frac{n_0^2-n_1^2}{a_0^2}\right)^{1/2}} \tag{213}$$

we have

$$\frac{d^2f}{d\xi^2} + (\sigma - \xi^2)f = 0 \tag{214}$$

which is the same differential equation of the form of the quantum harmonic oscillator. The modes of the square law media must be guided near the axis of the waveguide, which means

we require the function f to vanish as $x \to \infty$. The same requirement is imposed for the wave functions of the quantum harmonic oscillator. Bound solutions are met if we impose the condition

$$\sigma = 2p + 1. \tag{215}$$

This condition, together with (213), and with assigning the variable

$$b = \sqrt{\frac{a_o}{k_o(n_o^2 - n_1^2)^{\frac{1}{2}}}} \tag{216}$$

determine the possible values of the propagation constant β.

$$2p + 1 = \frac{(n_o^2 k_o^2 - \beta^2) a_o}{k_o(n_o^2 - n_1^2)^{\frac{1}{2}}}$$

$$2p + 1 = (n_o^2 k_o^2 - \beta^2) b^2$$

$$\beta_p = \sqrt{n_o^2 k_o^2 - \frac{(2p+1)}{b^2}}. \tag{217}$$

Returning to (214), the general solution is

$$f = H_p(\xi) e^{-\xi^2/2} \tag{218}$$

taking the appropriate derivatives

$$\frac{df}{d\xi} = \frac{dH_p}{d\xi} e^{-\xi^2/2} + H_p(-\xi) e^{-\xi^2/2}$$

$$\frac{d^2 f}{d\xi^2} = \frac{d^2 H_p}{d\xi^2} e^{-\xi^2/2} + \frac{dH_p}{d\xi}(-\xi) e^{0\xi^2/2} + \frac{dH_p}{d\xi}(-\xi) e^{-\xi^2/2} + H_p \left\{ (-\xi)(\xi) e^{-\xi^2/2} - e^{\xi^2/2} \right\}$$

$$\frac{d^2 f}{d\xi^2} = \frac{d^2 H_p}{d\xi^2} - 2\xi \frac{dH_p}{d\xi} + \xi^2 H_p e^{-\xi^2/2} - H_p e^{-\xi/2}. \tag{219}$$

Using the (215), (214) becomes

$$\frac{d^2 H_p}{d\xi^2} - 2\xi \frac{dH_p}{d\xi} + 2pH_p = 0 \tag{220}$$

which of the same form of (187), Hermite's Differential equation. Thus, the mode solutions for the quadratic index waveguide are the Hermite Gaussian functions, and these modes form a complete set of orthogonal functions. We can then describe every wave as a series expansion in terms of these modes.

From (208)

$$x^2 = \frac{\xi^2}{k_o \left(\frac{n_0^2 - n_1^2}{a_0^2}\right)^{1/2}} \tag{221}$$

$$x^2 = \frac{\xi^2}{k_o \left(\frac{n_0^2 - n_1^2}{a_0^2}\right)^{1/2}} \tag{222}$$

$$x^2 = \frac{\xi^2 w^2}{2} \tag{223}$$

and solving for ξ^2

$$\xi^2 = \frac{2x^2}{w^2} \tag{224}$$

and w^2 is

$$w^2 = \frac{2}{k_0 \left(\frac{n_0^2 - n_1^2}{a_0^2}\right)^{1/2}} \tag{225}$$

Using (224), the general solution to (214) can be expressed as

$$f = H_p(x) e^{-x^2/2} \tag{226}$$

and this can be expanded in a series expansion following the same procedure that derived (201). The trial solution (203) becomes

$$\phi(x,z) = \sum_{m=even}^{N} \frac{1}{\sqrt{\frac{1}{2}\left(\frac{b^2}{\sigma^2} + 1\right) \cdot 4^m m!}} \left(\frac{1-\rho^2}{\rho^2}\right)^m \cdot H_m(x) \cos(\beta_m z) e^{-x^2/2} \tag{227}$$

which gives the fields intensity profiles, or modes, of our planar quadratic index waveguide system. Figure 5 is the Octave simulation using (227), where the waveguide length is $32\mu m$, and the waveguide width is $10\mu m$.

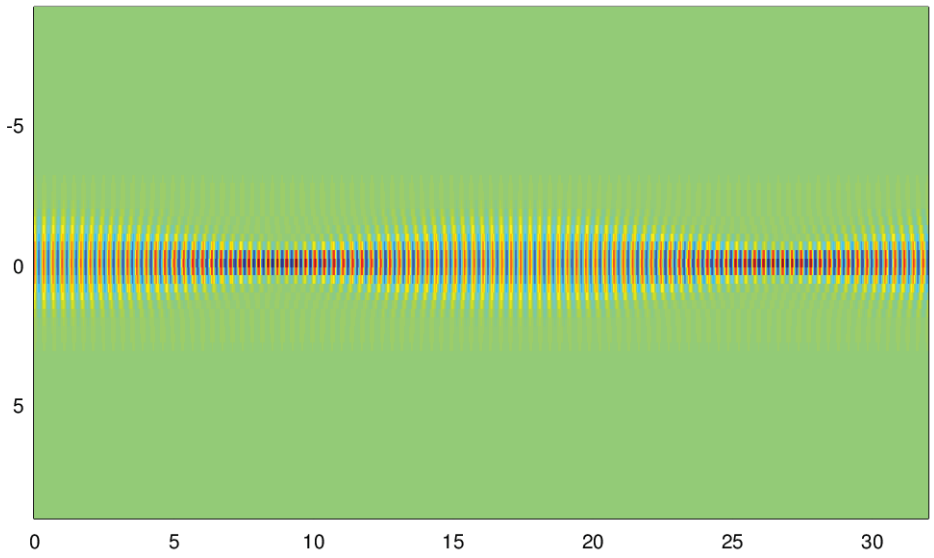

Figure 6: Simulation of field intensity profile from the analytic solution.

CHAPTER VI

NUMERICAL SOLUTIONS TO MAXWELL'S EQUATIONS

The Finite Difference Time Domain Method

The finite difference time domain (FDTD) method solves Maxwell's curl equations (Faraday's Law (36) and Ampere's Law (37) by discretizing space and time into finite rectangular grids. It uses central difference approximations, which has 2nd order accuracy, to 'propagate' equations (36) and (37) in time [14]. To obtain the central difference equations, first consider the Taylor series expansion of a function $f(z)$ expanded about the point z_0 with an initial offset $\pm\delta/2$

$$f(z_0+\delta/2) = f(z) + \frac{\delta}{2}\frac{df}{dz}|_{z=z_0} + \left(\frac{\delta}{2}\right)^2 \frac{d^2f}{dz^2}|_{z=z_0} + \frac{1}{3}\left(\frac{\delta}{2}\right)^3 \frac{d^3f}{dz^3}|_{z=z_0} + \cdots \tag{228}$$

$$f(z_0-\delta/2) = f(z) - \frac{\delta}{2}\frac{df}{dz}|_{z=z_0} + \left(\frac{\delta}{2}\right)^2 \frac{d^2f}{dz^2}|_{z=z_0} - \frac{1}{3}\left(\frac{\delta}{2}\right)^3 \frac{d^3f}{dz^3}|_{z=z_0} + \cdots . \tag{229}$$

Subtracting (229) from (228)

$$f(z_0+\delta/2) - f(z_0-\delta/2) = \delta\frac{df}{dz}|_{z=z_0} + \frac{2}{3!}\left(\frac{\delta}{2}\right)^3 \frac{d^3f}{dz^3} + \cdots \tag{230}$$

then dividing by the step size δ we have

$$\frac{f(z_0+\delta/2) - f(z_0-\delta/2)}{\delta} = f'(z_0) + \frac{1}{3!}\left(\frac{\delta}{2}\right)^2 f'''(z_0) + ... \tag{231}$$

where the prime indicate differentiation with respect to z. Rearranging, we solve for $f'(z)$

$$\frac{df}{dz}|_{z=z_0} = \frac{f(z_0+\delta/2) - f(z_0-\delta/2)}{\delta} + O(\delta^2). \tag{232}$$

and note that that the term $O(\delta^2)$ contains all the second-order and higher terms. If we choose a step size δ that is sufficiently small enough so that all terms in $O(\delta^2)$ are negligibly smaller than the first term on the right hand side, then we can make a reasonable

approximation for $df/dz|_{z=z_0}$ by dropping $O(\delta^2)$. We have for our approximation

$$\frac{df}{dz}|_{z=z_0} \approx \frac{f(z_0+\delta/2)-f(z_0-\delta/2)}{\delta}+O(\delta^2). \tag{233}$$

This is the central difference approximation for the derivative of the function at z_0. But the function is not sampled at z_0, but instead is sampled at the neighboring points $z_0+\delta/2$ and $z_0-\delta/2$.

For the simulations in this thesis, we consider the case for a wave traveling in the z-direction polarized in the x-direction. Faraday's law (36) is then

$$-\mu\frac{\partial\vec{\mathrm{H}}}{\partial t}=\nabla\times\vec{\mathrm{E}}=\hat{e}_y\frac{\partial E_x}{dz} \tag{234}$$

$$-\mu\frac{\partial H_y}{\partial t}=\frac{\partial E_x}{dz} \tag{235}$$

and Ampere's law (37) is

$$\epsilon\frac{\partial\vec{\mathrm{E}}}{\partial t}=\nabla\times\vec{\mathrm{B}}=-\hat{e}_x\frac{\partial H_y}{dz} \tag{236}$$

$$\epsilon\frac{\partial E_x}{\partial t}=\frac{\partial H_y}{dz}. \tag{237}$$

We now introduce notation to identify the spatial and temporal step of the fields. For E_x, we will use $E_x(z,t)=E_x^p(q)$, and for H_y we will use $H_y(z,t)=H_y^p(q)$ where p indicates the temporal step, and q indicates the spatial step.

To find the value of H_y, a the next one-half spatial step $((q_1/2)\Delta z, p\Delta t)$ we use Faraday's law

$$-\mu\frac{H_y^{p+1/2}(q+1/2)-H_y^{p-1/2}(q+1/2)}{\Delta t}=\frac{E_x^p(q+1)-E_x^p(q)}{\Delta z}. \tag{238}$$

Solving for $H_y^{p+1/2}(q+1/2)$, we obtain the update equation for H_y

$$H_y^{p+1/2}(q+1/2)=H_y^{p-1/2}(q+1/2)-\frac{\Delta t}{\mu\Delta z}\left[E_x^p(q+1)-E_x^p(q)\right]. \tag{239}$$

The corresponding update equation for E_x is obtain from Ampere's law using the same

procedure. The central-difference approximation is

$$\epsilon \frac{E_x^{p+1}(q) - E_x^p(q)}{\Delta t} = \frac{H_y^{+1/2}(q+1/2) - H_y^{p+1/2}(q-1/2)}{\Delta z}. \tag{240}$$

Solving for $E_x^{p+1}(q)$, we have

$$E_x^{p+1}(q) = \frac{\Delta t}{\epsilon \Delta z}\left[H_y^{p+1/2}(q+1/2) - H_y^{p+1/2}(q-1/2)\right] \tag{241}$$

These equations calculate the electric and magnetic fields in 1/2 increments, known as the *leapfrog method*, in which the electric field is calculated in a unit grid volume, then the magnetic field is calculated in the same unit grid volume, but at the next time step. The FDTD first calculates the electric field for the entire space at the first time step, then the magnetic fields for the entire space in the next time step. In other words, it solves the initial value problem where the fields and currents are zero for $t < 0$, then non-zero values evolve in response to some currents, or sources.

MEEP

MEEP is a FDTD solver that simulates Maxwell's curl equations. MEEP is used to calculate field intensity profiles in computational electromagnetic problems [12]. It uses the *Yee grid* discretization to divide space and time into regular finite rectangular grids. In this grid, each field component is sampled at difference spatial locations offset by a half-pixel using the center-difference calculation of space and time. A 2D illustration of the Yee grid is shown in Figure 7. The time derivative of the vector field H produces an electric field around it as predicted by Faraday's Law. And as predicted by Ampere's Law, the time derivative of the electric field produces the curl of the vector field H around it. In MEEP, the electric field and vector field H are initially zero at $t = 0$. The fields are calculated as time increases, and the fields are found to be non-zero because of their interaction with a source, and in our simulation, a Gaussian laser beam.

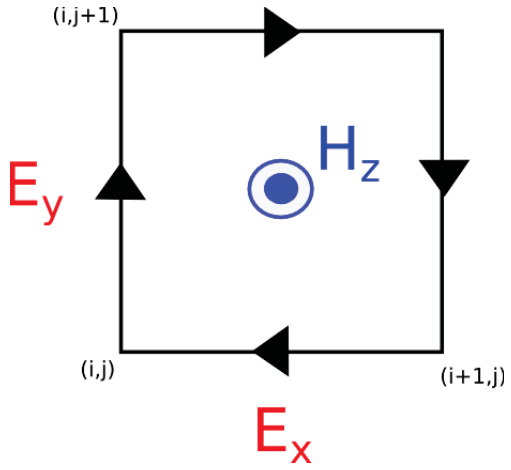

Figure 7: Yee grid, in 2D.

MEEP uses the scripting language Scheme. Scheme differs in syntax from MatLab and Octave in unique ways. For example, in Octave to perform the operation 4 minus 5, one would implement this as

$(4-5)$

but in Scheme, this is implemented as

$(-\ \ 4\ \ 5)$.

A Gaussian distribution

$$f(y) = \frac{y^2}{2\sigma^2} \tag{242}$$

can be implemented in MEEP as

```
(exp (/(* -1 (vector3-y spoint) (vector3-y spoint)) (* 2 sourcesigma sourcesigma))))
```

where σ is the variance (or spread) of the distribution.

Users can write scripts to define parameters, computational cell sizes, geometries, and sources of the simulation. Access to the source code allows flexibility to the user not seen in GUI-based or CAD-based FDTD packages.

MEEP uses dimensionless units, $\epsilon_o = \mu_o = c = 1$. This emphasizes the scale invariance of Maxwell's equations, and the fact that most meaningful quantities are almost always dimensionless ratios (such as scattered power over incident power). MEEP allows the user to choose a lengthscale a, then all distances are given in units of a. All times are in units a/c,

and all frequencies are in units c/a, or equivalently a/λ, where λ is the vacuum wavelength. Relative permitivity and permeability constants can be defined in MEEP.

Boundary conditions can be defined and MEEP, and in the MEEP simulation used in this thesis the *perfectly matched layers* (PML) boundary condition is used. This simulates open boundary conditions by absorbing all waves incident on it, and does not allow reflections. Strictly speaking, this is not a 'boundary condition'. Rather, it is a fictitious absorbing material. The PML is given some finite thickness that causes the fictitious material to gradually turn on. This is because in an actual discretized system, the PML material has some small reflections.

MEEP Simulation

To simulate wave propagation in quadratic index waveguides using MEEP, we first define the computational cell, which can also be interpreted as the dimensions of our waveguide. Then we define the refractive indices along the optical axis and boundary, and define a continuous Gaussian beam source. Defining x as the transverse dimension, a Gaussian distribution is

$$f(x) = e^{-x^2/2\sigma^2} \tag{243}$$

where σ is the variance of the distribution, and in this simulation is equal to 1.

The frequency was defined to equal $\nu = 1.5$. If a lengthscale of $a = 1\mu m$ is used, then the wavelength is $\lambda = a/\nu = 1\mu m/1.5 = 0.667\mu m$ or $667nm$. A half-waveguide width a_o was defined to equal $5\mu m$, and the long-axis waveguide dimension is $32\mu m$. These dimensions were chosen to match the Gaussian ray bundle simulation.

The MEEP simulation of a Gaussian beam in a planar quadratic index waveguide was performed using PML boundary's, and an initial beam waist size of $10\mu m$. The index profile is of the form of equation (1).

Figure 8: Index profile simulation in MEEP.

The simulation yields the following intensity profile

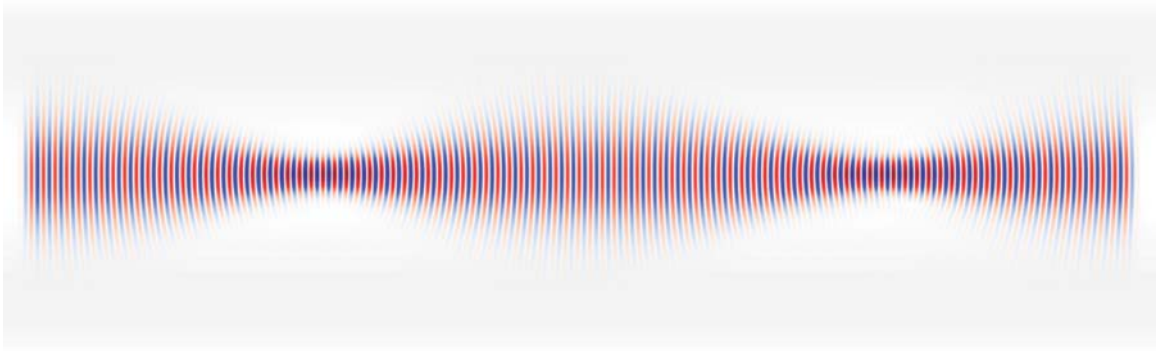

Figure 9: MEEP simulation of a Gaussian beam in a quadratic index waveguide.

The corresponding grayscale image is

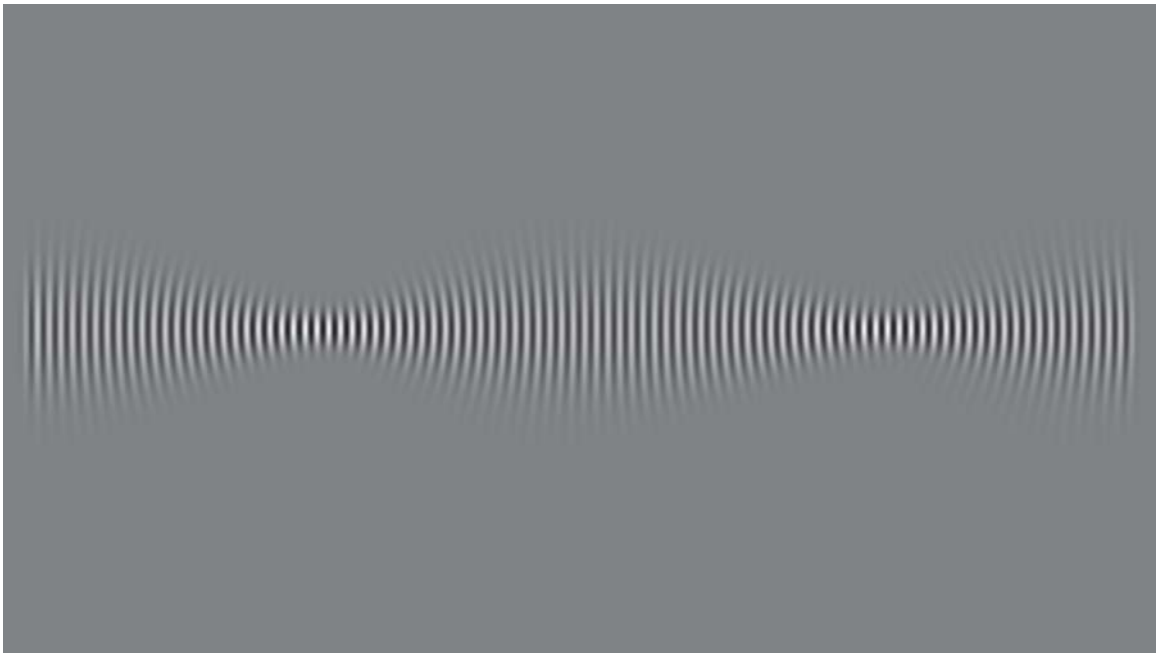

Figure 10: Grayscale image of MEEP simulation for a Gaussian beam in a quadratic index waveguide.

Comparison of MEEP and Analytic Simulations

This sections shows plots that compare the analytic solution to the Helmholtz wave equation to the simulation results obtain from MEEP. These are graphical comparisons comparing the grayscale pixel intensities of the two simulation. Two plots are shown, one comparing the MEEP simulation with the analytic solution up to 2nd order, and the other using the analytic solution up 20th order. Currently, results are seen to agree only through the first cycle. After that, the two simulations are out of phase.

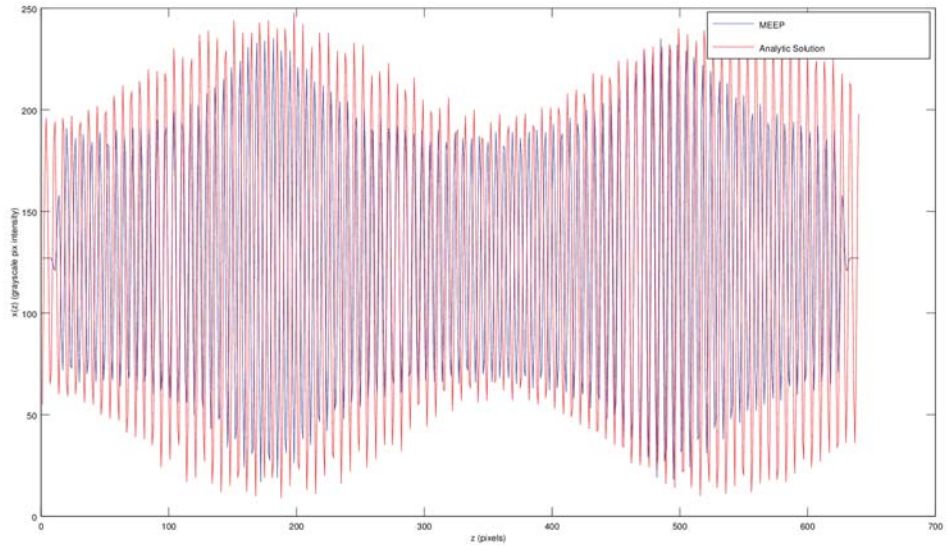

Figure 11: Comparison of MEEP simulation with analytic solution expansion up to 2nd order.

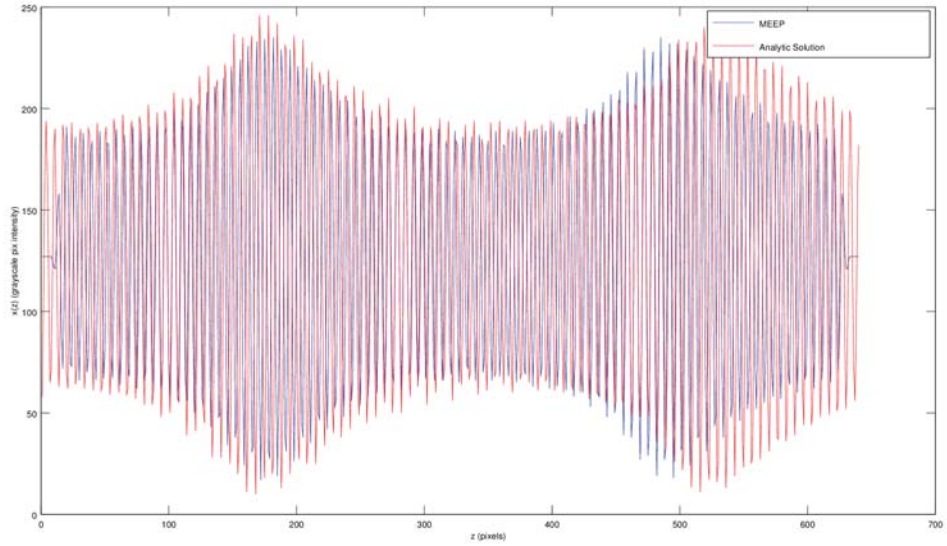

Figure 12: Comparison of MEEP simulation with analytic solution expansion up to 20th order.

CHAPTER VII

COMPARISON OF GAUSSIAN RAY BUNDLES WITH THE NUMERICAL SOLUTIONS TO MAXWELL'S EQUATIONS AND THE ANALYTIC SOLUTIONS OF THE SCALAR WAVE EQUATION

Here the analytic solution to Hamilton's equations for a Gaussian bundle of ray trajectories will be graphically compared to the analytic solution to the Helmholtz wave equation. Instead of using the signed field intensity solution, we want to use the time-average field intensity. To find the time-average field intensity

$$I = \frac{e^{-x^2/2}}{T} \int_0^T \phi(x,z)^* \phi(x,z) dt \tag{244}$$

Going out to 2nd order

$$I = \frac{e^{-x^2/2}}{T} \int_0^T \left(C_0 H_0 e^{-i\beta_0 z} + C_2 H_2 e^{-i\beta_2 z} \right) e^{i\omega t} \left(C_0 H_0 e^{i\beta_0 z} + C_2 H_2 e^{i\beta_2 z} \right) e^{-i\omega t} dt \tag{245}$$

$$I = \frac{e^{-x^2/2}}{T} \left(C_0^2 H_0^2 e^{-i(\beta_0 - \beta_0)z} + 2C_0 C_2 H_0 H_2 e^{-i(\beta_0 - \beta_2)z} + C_2^2 H_2^2 e^{-i(\beta_2 - \beta_2)z} \right) \int_0^T e^{-(\omega-\omega)t} dt. \tag{246}$$

The time dependent integral equals T, and the exponential factors of the squared terms vanish, and we're left with

$$I = e^{-x^2/2} \left\{ C_0^2 H_0^2 + 2C_0 C_2 H_0 H_2 e^{-i(\beta_0 - \beta_2)z} + C_2^2 H_2^2 \right\}. \tag{247}$$

The generalized expression for the time-average field intensity for even orders n is

$$I = e^{-x^2/2} \left\{ \sum_{n=0}^{N} \phi_n^2 + 2 \sum_{n=0}^{N} \sum_{m=n+2}^{N} \phi_n \phi_m \cos\left(\left(\beta_n - \beta_m \right) z \right) \right\}. \tag{248}$$

The generalized field intensity was simulated in Octave. Figure 13 is the simulation up to 2nd order, and Figure 14 is the simulation up to 20th order. We see that taking the expansion to higher orders increases the accuracy of the simulation, producing a more *real* looking beam that we would expect to see in experiment

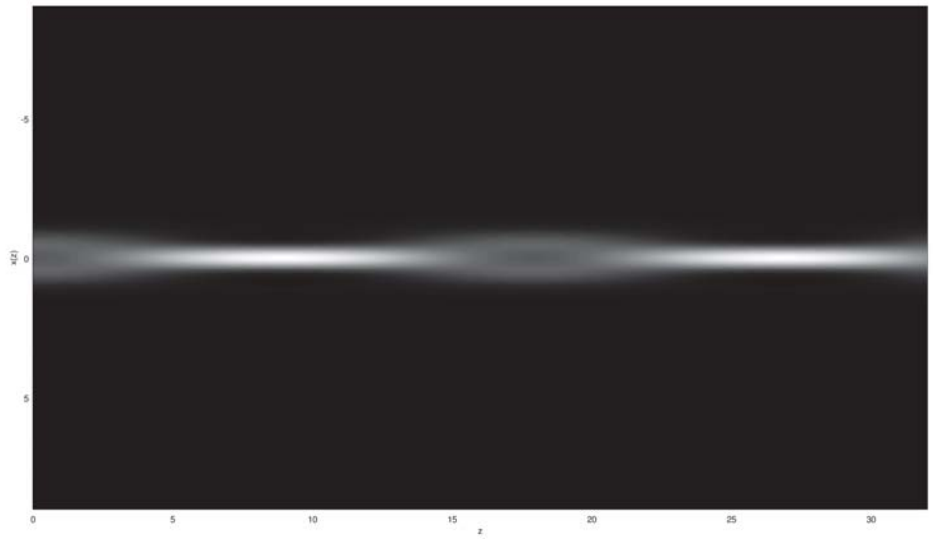

Figure 13: Time-average field intensity for the analytic solution to the Helmholtz equation for order n=2.

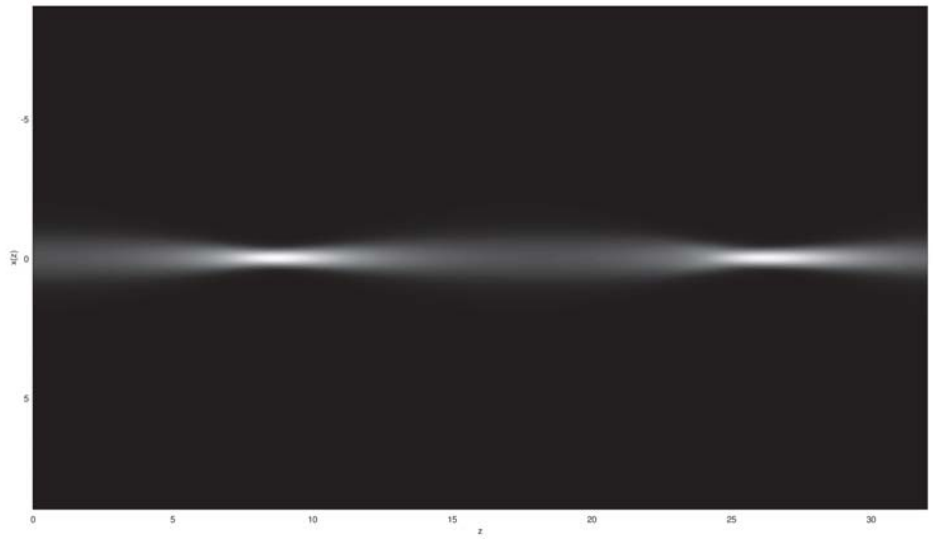

Figure 14: Time-average field intensity for the analytic solution to the Helmholtz equation for order n=20.

Next we wish to compare the Gaussian ray bundle with the average field intensity. Figure 15 is a plot overlaying the Gaussian ray bundles trajectories over the average field intensity plot.

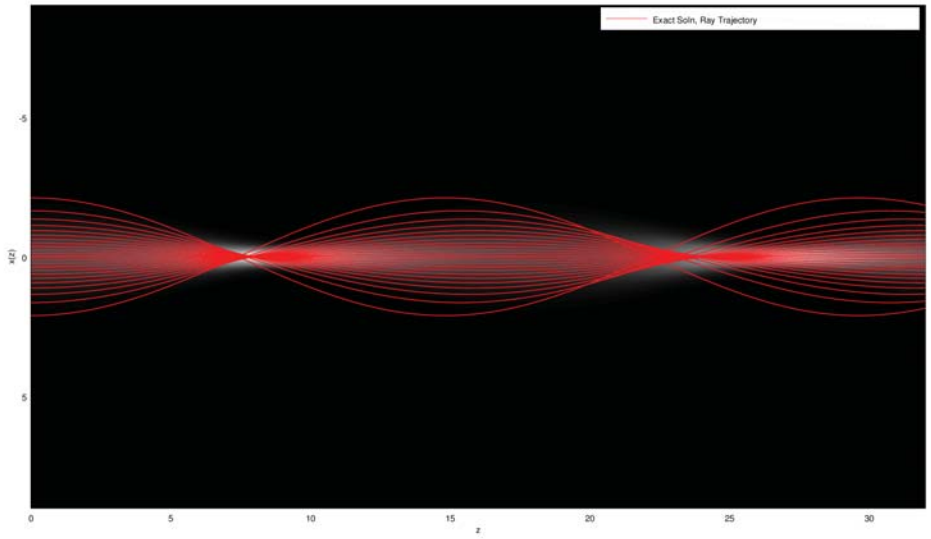

Figure 15: Comparison of analytic solution of Gaussian ray bundle trajectories with time-average field intensity of analytic solution simulation up to 20th order.

CHAPTER VIII
FUTURE WORK

This chapter describes future work on the analysis presented in this thesis, and problems that will use all of the theory and simulation techniques used in this thesis. It's suggested that we can make predictions about the field intensity from the Gaussian ray bundle analysis. An exact agreement wasn't seen graphically, but future work would include quantifying how the focus regions of the field intensities correspond with the nodes created by the Gaussian ray bundle trajectories on the optical axis.

Simulating a Gaussian beam in planar quadratic index waveguides was performed by expanding a Gaussian function in terms of Hermite polynomials. But it is also suggested by Macuse [11] that there exists a closed-form solution for the modes in a square law medium. Its proposed that this closed form solution can be verified by the same methods used in this thesis, and a comparison to the series expansion can be made to reveal any potential disagreements between the two solutions.

The comparisons between solution of scalar wave equation and the numerical solutions to Maxwell's equations from MEEP also required more detail investigation. The analytic solution to the scalar wave equation was obtain by imposing paraxial approximations, whereas the simulations performed in MEEP is a full vectorial wave simulation of Maxwell's Equations. How do these differ, and how can these differences be quantified? If these differences are understood, we can then make accurate prediction of ray propagation from the field intensity profiles.

The theoretical development and simulations presented in this thesis can also be applied to systems involving electromagnetic light propagation with spatially varying medium where an analytic solution does not exist. One such system is a planar quadratic index waveguide with periodic axial perturbations. The numerical simulations, verified by comparison with analytic solutions, can be used to simulate light propagation in this system, and to determine the conditions that predict chaotic ray behavior.

REFERENCES

[1] SS Abdullaev and GM Zaslavskiĭ. Classical nonlinear dynamics and chaos of rays in problems of wave propagation in inhomogeneous media. *Soviet Physics Uspekhi*, 34(8):645, 1991.

[2] M. Asadi-Zeydabadi and R. P. Tagg. Ray chaos in media with transversal and axial variation of index of refraction: Linear stability.

[3] M. Asadi-Zeydabadi and R. P. Tagg. Parametric instability in waveguides with axial modulation of the index of refraction. *PhD Dissertation, University of Colorado Boulder*, 2004.

[4] SS Bayin. Mathematical methods in science and engineering. 2006. *John Wiley&Sons, New York*, page Chapter 4.

[5] Josselin Garnier. Light propagation in square law media with random imperfections. *Wave Motion*, 31(1):1–19, 2000.

[6] AK Ghatak and EG Sauter. The harmonic oscillator problem and the parabolic index optical waveguide: I. classical and ray optic analysis. *European Journal of Physics*, 10(2):136, 1989.

[7] David Jeffrey Griffiths and Edward G Harris. *Introduction to quantum mechanics*, volume 2. Prentice Hall New Jersey, 1995.

[8] M Hashimoto. Geometrical optics of guided waves in waveguides. *Progress In Electromagnetics Research*, 13:115–147, 1996.

[9] Herwig Kogelnik. On the propagation of gaussian beams of light through lenslike media including those with a loss or gain variation. *Applied Optics*, 4(12):1562–1569, 1965.

[10] S Longhi, G Della Valle, and D Janner. Ray and wave instabilities in twisted graded-index optical fibers. *Physical Review E*, 69(5):056608, 2004.

[11] Dietrich Marcuse. *Light Transmission Optics*. 1982.

[12] Ardavan F Oskooi, David Roundy, Mihai Ibanescu, Peter Bermel, John D Joannopoulos, and Steven G Johnson. Meep: A flexible free-software package for electromagnetic simulations by the fdtd method. *Computer Physics Communications*, 181(3):687–702, 2010.

[13] JS Shirk, M Sandrock, D Scribner, E Fleet, R Stroman, E Baer, and A Hiltner. Biomimetic gradient index (grin) lenses. Technical report, DTIC Document, 2006.

[14] A Taflove and KR Umashankar. The finite-difference time-domain (fd-td) method for electromagnetic scattering and interaction problems. *Journal of Electromagnetic Waves and Applications*, 1(3):243–267, 1987.

[15] Qi Wu, Jeremiah P Turpin, and Douglas H Werner. Integrated photonic systems based on transformation optics enabled gradient index devices. *Light: Science & Applications*, 1(11):e38, 2012.

APPENDIX A

Code: Analytic Solution for Ray Trajectories

```
%%%%%%%%%%EXACT_SOLN_MAIN.M
%uses function 'qdinxexact.m'
%
%
n0=4; %center line index (optical axis)
n1=1; %index at the boundary
a0=5; %waveguide distance from center
z0=0;
zf=32; %waveguide length
theta0_degs=0; %initial angle, in degrees
xstart=1.25; %initial transverse position
while xstart>=-1.25
        theta0_rads=theta0_degs*(3.14159/180); %convert initial angle to radians
        theta0=theta0_rads;
        [x_z]=qdinxexact(n0,n1,a0,z0,zf,xstart);
        z=linspace(z0,zf,2000);
        xlabel('z');
        ylabel('x(z)');
        plot(z,x_z,'r-','LineWidth',2);
        legendexact=legend('Exact Soln');
        hold on
        xstart=xstart-.25;
end

function [x_z]=qdinxexact(n0,n1,a0,z0,zf,xstart)

z=linspace(z0,zf,2000);
lambda=2*pi*a0*sqrt(n0^2/(n0^2-n1^2)-(xstart/a0)^2);
x_z=xstart*cos((2*pi*z)/lambda); %general equation for ray trajectories
end
```

APPENDIX B

Code: Hamilton's Equations Solved Using `ode45`

```
%%%%%%%%%%%%%%%%HAMILTONS_EQNS_RAYPATHS.M
%Uses ode45 to solve Hamilton's equation
%to determine ray trajectories in a planar
%quadratic index waveguide.
%
%
%
n0=4; %center line index (optical axis)
n1=1; %index at the boundary
a0=5; %waveguide distance from center
z0=0;
zf=32; %waveguide length
theta0_degs=0; %initial angle, in degrees
theta0_rads=theta0_degs*(3.14159/180); %convert initial angle to radians
theta0=theta0_rads;
p0=n0*sin(theta0);
options=[n0,n1,a0,theta0];
xinit=1.25; %initial transverse position
while xinit >=-1.25

        x0=[xinit,p0];
        t=z0:0.02:zf;
        [z,x]=ode45(@raypath,t,x0,options);
        xx=x(:,1);
        p=x(:,2);
        plot(z,xx,'b-','LineWidth',2)
        legend2=legend('Hamiltons Equations solved by ode45');
        hold on
        xinit=xinit-0.25;
end

function dy = raypath(t,x0,options)

n0=options(1);
n1=options(2);
a0=options(3);
theta0=options(4);

if isreal(x0)
xx=x0(1);
p=x0(2);
else
    return
end

n=sqrt(n0^2-(n0^2-n1^2)*(xx^2/a0^2));
dn=-((n0^2-n1^2)*(xx/a0^2));
dx=p/(sqrt(n^2-p^2));
dp=(dn)/(sqrt(n^2-p^2));
dy=[dx;dp];
p0=n*sin(theta0);
end
```

APPENDIX C

Code: Gaussian Ray Bundle

```
%%%%%%%%%%GAUSSIAN_RAY_BUNDLE.M
%Simulates the trajectories of a Gaussian ray bundle
%Uses function 'qdinxexact.m'
%
%
n0=4; %center line index (optical axis)
n1=1; %index at the boundary
a0=5; %waveguide distance from center
z0=0;
zf=32; %waveguide length
theta0_degs=0; %initial angle, in degrees

spacing=0.12; %spacing between on-axis ray and adjacent rays. Determines # of rays

raydist(1)=0;

alpha1=spacing;
raydist(2)=alpha1;
raydist(3)=raydist(2)+alpha1*e^(raydist(2)^2/2);

irays=3;

rayflag=0;
while rayflag==0
        raydist(irays+1)=raydist(irays)+alpha1*e^(raydist(irays)^2/2);
        irays=irays+1;
        if raydist(irays)>a0
                raydist(irays)=[];
                rayflag=1;
        end
end
raydist(length(raydist))=[];
raydist;

maxnumrays=length(raydist)
for iray=1:maxnumrays
        xstart=raydist(iray);
        theta0_rads=theta0_degs*(3.14159/180); %convert initial angle to radians
        theta0=theta0_rads;
        [x_z]=qdinxexact(n0,n1,a0,z0,zf,xstart);
        z=linspace(z0,zf,2000);
        xlabel('z');
        ylabel('x(z)');
        plot(z,x_z,'r-','LineWidth',1);
        legendexact=legend('Exact Soln, Ray Trajectory');
        hold on
end

%now switch sign of inital ray postions, for other 'half' of gaussian ray bundle
for iray=1:maxnumrays
        xstart=-raydist(iray);
        theta0_rads=theta0_degs*(3.14159/180); %convert initial angle to radians
        theta0=theta0_rads;
```

```
        [x_z]=qdinxexact(n0,n1,a0,z0,zf,xstart);
        z=linspace(z0,zf,2000);
        xlabel('z');
        ylabel('x(z)');
        plot(z,x_z,'r-','LineWidth',1);
        legendexact=legend('Exact Soln, Ray Trajectory');
        hold on
end
```

APPENDIX D

Code: Analytic Solution to the Scalar Wave Equation

```
%%%%%%%%%%%%%%%%%%%%%%%%%%%%%%%%%%%%%%%%%%%%%%%%%%%%%%%%%%%%%%%%%%%%%%%%%%%%%%%%
%%MAIN SCRIPT FOR ANALYTIC SOLN, WAVE EQUATION IN SQUARE LAW MEDIUM
%%Required functions: bbeta.m, hermitecoeffs.m, mfac.m, EE004.m,
%%calcexpancoeffs.m, evalinten.m
%%
%
%
%
%
%
%
%
clear all
nn=20 %Hermite polynomial order, must be even
iorder=nn;

iorderdiv=iorder/2;
m=0:1:iorderdiv;


%%%%%%%%%%%%%%%%Waveguide dims

%For comparison with MEEP simulation
y=-9:0.03:9; %change step size to increase resolution of images
z=0:0.02:32;

%Parameters
a0=5.0; %Waveguide half width

%For comparison with MEEP simulation
n0=4.0; %center index of refraction
n1=1.0; %boudary index of refraction

sourcesigma=1.0;
frequency=1.5; %This is meep's dimensionless frequency

wavelength=1/frequency;
k0=2*pi/wavelength;
b=sqrt(a0/(k0*sqrt(n0-n1)));  %The natural scale
ggamma=sqrt(0.5*((b/sourcesigma)^2+1));
ggugga=(1-ggamma^2)/ggamma^2;


propconst=bbeta(m,n0,b,k0,iorder);

fac=mfac(m,ggamma,ggugga); %expansion coefficients
eeta=y/b; % y dimension divided by natural scale
x=eeta';%Used to evaluate each Hermite polynomial

function H_0=H0(x)
        H_0=x;
        H_0(:)=1; %lowest order Hemite polynomial is 1 (single row)
end
```

```
ihermitepolys=1;
while iorder > 0
        coeffs=hermitecoeffs(iorder);
        numofcoeffs=length(coeffs);
        istep=1;
        while istep < numofcoeffs
                if coeffs(istep)==0
                        coeffs(istep)=[];
                        numofcoeffs=numofcoeffs-1;
                end
        istep=istep+1;
        end
        coeffs;
        numofcoeffs=length(coeffs);

        ipwr=iorder;
        for icoeffs=1:numofcoeffs
                coeffs(icoeffs); %debug point
                term(:,icoeffs)=coeffs(icoeffs).*(x.^ipwr); %numerically calc each term
                ipwr=ipwr-2;
                if ipwr < 0
                        msg='ipwr below condition'; %debug pt
                        break
                end
        end
        H.(num2str(ihermitepolys))=term;
        term(:,(numofcoeffs-1))=[];
        ihermitepolys=ihermitepolys+1;
        iorder=iorder-2;
end

%%%%%%All H's evaluated with eeta'
struct_levels_to_print(0) %adjust the argument to see specific fields of structure
H;
H_0=H0(x);
iorder=nn;
[yy,inten]=EE004(y,z,b,m,fac,propconst,x,H,H_0,iorder,a0);
[TimeAvgIntensity,crossfield,sqrdfield]=evalinten(inten,iorder,propconst,z,x,fac);
imagesc(z,y,TimeAvgIntensity) %to plot time-avg field intensity
%imagesc(z,y,yy)%to plot signed field intensity
colormap(gray)
xlabel('z')
ylabel('x(z)')
hold on


function propconst=bbeta(m,n0,b,k0,iorder)
        iter=0;
    im=1;
    while iter <=iorder
        propconst(im)=sqrt(k0.^2*n0-(2*iter+1)/b.^2);
        iter=iter+2;
        im=im+1;
    end
endfunction
```

```
function  fac=mfac(m,ggamma,ggugga)
        fac=ggugga.^m./(ggamma*4.^m.*gamma(m+1));
endfunction


function hk = hermitecoeffs(n)

if n==0
    hk = 1;
elseif n==1
    hk = [2  0];
else
    hkm2 = zeros(1,n+1);
    hkm2(n+1) = 1;
    hkm1 = zeros(1,n+1);
    hkm1(n) = 2;
    for k=2:n
        hk = zeros(1,n+1);
        for e=n-k+1:2:n
            hk(e) = 2*(hkm1(e+1) - (k-1)*hkm2(e));
        end
        hk(n+1) = -2*(k-1)*hkm2(n+1);
        if k<n
            hkm2 = hkm1;
            hkm1 = hk;
        end
    end
end


function [yy,inten]=EE004(y,z,b,m,fac,propconst,x,H,H_0,iorder,a0)
        numofpolys=length(propconst);
        yy=fac(1)*H_0*cos(propconst(1)*z); %lowest order of expansion
        inten.(num2str(1))=fac(1)*H_0;
        struct_levels_to_print(0)
        iinten=2;%index for intensity struct
        ifac=2; %index to calc expansion coefficient
        ibeta=2;%index to calc propagation constant
        a=fieldnames(H);
        iherm=length(a);%starts at Hermite order n=2, should be the (row)x2 (2 columns) matrix in H
        hn=0; %create variable to store evaluated expansion terms
        while (iherm > 0)
                Hn=(H.(num2str(iherm)));
                icols=length(Hn(1,:)); %number of columns in the struct field
                while (icols >=2)
                        if (rem(icols,2)==0)% if number of columns is even
                                hn=hn+Hn(:,icols)+Hn(:,icols-1); %add last two columns
                                icols=icols-2; %subtract last two columns
                        elseif (rem(icols,2)==1)% && (icols >1) %if number of columns is odd
                                hn=hn+Hn(:,icols);
                                icols=icols-1;
                        endif

                endwhile %Have now evaulated each term for the current Hermite polynomial order
                inten.(num2str(iinten))=fac(ifac)*hn;
                yy=yy+fac(ifac)*hn*cos(propconst(ibeta)*z);
```

```
                hn=0;%reset variable
                iinten=iinten+1;
                ifac=ifac+1;
                ibeta=ibeta+1;
                iherm=iherm-1;
        endwhile
        moo=z;
        moo(:)=1;
        yy=(exp(-0.5*x.^2).*moo).*yy;
endfunction


function [TimeAvgIntensity,crossfield,fieldsqrd]=evalinten(inten,iorder,propconst,z,x,fac)
moo=z;
moo(:)=1;
intenfieldnames=fieldnames(inten);
N=length(intenfieldnames)
fieldsqrd=0;
ifieldsqrd=1;
while ifieldsqrd <= N
        fieldsqrd=fieldsqrd+(inten.(num2str(ifieldsqrd)).^2); %Sums all of the squard terms
        ifieldsqrd=ifieldsqrd+1;
end
%fieldsqrd=(exp(-0.5*x.^2).*moo).*fieldsqrd;

field=0;
ifield=1;
while ifield <=N
        ifieldnxt=ifield+1;
        while ifieldnxt<=N
                betadiff=propconst(ifield)-propconst(ifieldnxt);
                crossfield=2*inten.(num2str(ifield)).*inten.(num2str(ifieldnxt))*cos((betadiff)*z);%Sums all of the
                field= field + crossfield;
                ifieldnxt=ifieldnxt+1;
        end
        ifield=ifield+1;
end
%field;
intensum=(exp(-0.5*x.^2).*moo).*fieldsqrd + (exp(-0.5*x.^2).*moo).*field;
TimeAvgIntensity=(exp(-0.5*x.^2).*moo).*intensum;
end
```

APPENDIX E.

Code: MEEP Simulation

```
(define mypoint (vector3 0 0 0))
(define spoint (vector3 0 0 0))
(define a0 5.0)  ; waveguide half-width
(define eps0 4)  ; center-line dielectric constant
(define eps1 1)  ; edge dielectric constant
(define sourcesize 10.0); size of initial full beam waist
(define sourcesigma 1.0); variance of Gaussian distribution
(set! geometry-lattice (make lattice (size 32 18 no-size)))
;;;;;;;;;;;;;;;

(define (epsfunc mypoint) (make dielectric (epsilon (if (> (vector3-y mypoint) a0) eps1
   (- eps0 (* (- eps0 eps1) (/ (* (vector3-y mypoint) (vector3-y mypoint)) (* a0 a0))))))))



(set! geometry (list
                (make block (center 0 0) (size infinity 10 infinity)
                      (material (make material-function (material-func epsfunc))))))

(define (gaussprof spoint)
    (exp (/(* -1 (vector3-y spoint) (vector3-y spoint)) (* 2 sourcesigma sourcesigma))))

(set! sources (list
               (make source
                 (src (make continuous-src (frequency 1.5)))
                 (component Ez)
                 (center -15 0)
                 (size 0 sourcesize)
                 (amp-func gaussprof))))

;;;;;;;;;;;;;;;;;;;;;;
(set! pml-layers (list (make pml (thickness 1.0))))
(set! resolution 20)
(run-until 200
           (at-beginning output-epsilon)
           (at-end output-efield-z))
```

APPENDIX F

The Quantum Harmonic Oscillator

Introduction

The quantum harmonic oscillator is a system which can be solved analytically and has significant importance in physics. The analytical solution of the quantum harmonic oscillator also describes other quantum mechanical systems such as wave propagation in an enclosure. The quantum mechanical behavior of the wave function at infinity from determined eigenvalues and their corresponding eigenfunctions and for angular momentum operators will provide the basis to which such systems can be analyzed [7].

The Schrodinger Wave Equation

In quantum mechanics, the behavior of a particle is described by a wave function $\Psi(x,t)$ (here in 1D), and this wave function is a solution to the Schrodinger wave equation

$$i\hbar\frac{\partial\Psi}{\partial t} = -\frac{\hbar^2}{2m}\frac{\partial^2\Psi}{\partial x^2} + V\Psi \tag{249}$$

where V is the potential energy of the system and $\hbar$ is Plank's constant

$$\hbar = \frac{h}{2\pi} = 1.054573x10^{-34}Js. \tag{250}$$

The Schrodinger equation allows us to find $\Psi(x,t)$ for all future times if we are given appropriate initial conditions.

The Statistical Interpretation of the Wave Function

The wave function gives the probability of locating a particle at some specified time. But it does not tell us where exactly the particle is located in x, but rather that the particle's location is a function of x. Max Born proposed a statistical interpretation of the wave function to allow us to describe the state of the particle in space and time. Born proposed that $|\Psi(x,t)|^2$ gives the probability of finding the particle at a location x at time t.

The Time-Independent Schrodinger Equation

The Schrodinger equation can be used to find the wave function $\Psi(x,t)$ using separation of variables, assuming the potential V is independent of time. The solutions are of the form

$$\Psi(x,t) = \psi(x)f(t) \tag{251}$$

where ψ is a function of x alone, and f is a function of t alone. Taking the derivatives

$$\frac{\partial \Psi}{\partial t} = \psi \frac{df}{dt}, \quad \frac{\partial^2 \Psi}{\partial x^2} = \frac{d^2\psi}{dx^2} f \tag{252}$$

the Schrodinger equation becomes

$$i\hbar \frac{1}{f}\frac{df}{dt} = -\frac{\hbar^2}{2m}\frac{1}{\psi}\frac{d^2\psi}{dx^2} + V. \tag{253}$$

The left side of (253) is a function of t of alone, and the right side is a function of x alone. This holds only if both sides are constant. We then set the left and right hand sides equal to a separation constant E

$$\frac{df}{dt} = -\frac{iE}{\hbar} f, \tag{254}$$

and

$$-\frac{\hbar^2}{2m}\frac{d^2\psi}{dx^2} + V\psi = E\psi. \tag{255}$$

Separation of variables has turned a partial differential equation into two ordinary differential equations (254) and (255). Equation (255) is the time-independent Schrodinger equation and its general solution is $C\exp(-iEt/\hbar)$. The constant C can be absorbed into ψ since the quantity of interest is the product ψf. Then

$$f(t) = e^{-iEt/\hbar}. \tag{256}$$

The Quantum Harmonic Oscillator

The potential for the quantum harmonic oscillator is

$$V(x) = \frac{1}{2}m\omega^2 x^2 \tag{257}$$

and the time-independent Schrodinger equation becomes

$$-\frac{\hbar^2}{2m}\frac{d^2\psi}{dx^2} + \frac{1}{2}m\omega^2 x^2\psi = E\psi. \tag{258}$$

Analytic Solution based on Hermite Polynomials

To solve (258), we rewrite it in terms of a dimensionless variable

$$\zeta \equiv \sqrt{\frac{m\omega}{\hbar}}x. \tag{259}$$

The Schrodinger equation then becomes

$$\frac{d^2\psi}{d\zeta^2} = \left(\zeta^2 - K\right)\psi \tag{260}$$

where K is the energy in units of $(1/2)\hbar\omega$ and is equal to $K \equiv \frac{2E}{\hbar\omega}$. Solving (260) gives the allowed values of K, and the corresponding energy values E.

For very large ζ and x, the constant K dominates ζ^2

$$\frac{d^2\psi}{d\zeta^2} \approx \zeta^2\psi \tag{261}$$

which has the approximate solutions

$$\psi(\zeta) \approx Ae^{-\frac{\zeta^2}{2}} + Be^{+\frac{\zeta^2}{2}}. \tag{262}$$

For $x \to \infty$, The B term blows up and the physically acceptable solutions have an asymptotic form given by

$$\psi(\zeta) \to De^{-\frac{\zeta^2}{2}}. \tag{263}$$

Differentiating (263)

$$\frac{d\psi}{d\zeta} = \left(\frac{dh}{d\zeta} - \zeta h\right) e^{-\frac{\zeta^2}{2}} \tag{264}$$

and taking the second derivative

$$\frac{d^2\psi}{d\zeta^2} = \left(\frac{d^2h}{d\zeta^2} - 2\zeta\frac{dh}{d\zeta} + (\zeta^2 - 1)h\right) e^{-\frac{\zeta^2}{2}} \tag{265}$$

the Schrodinger equation is then

$$\frac{d^2h}{d\zeta^2} - 2\zeta\frac{dh}{d\zeta} + (K-1)h = 0. \tag{266}$$

To find solutions to (266), we expand $h(\zeta)$ in a power series

$$h(\zeta) = a_0 + a_1\zeta + a_2\zeta^2 + \cdots = \sum_{j=0}^{\infty} a_j\zeta^j. \tag{267}$$

Taking the first derivative of the series term by term we have

$$\frac{dh}{d\zeta} = a_1 = 2a_2\zeta + 3a_3\zeta^2 + \cdots = \sum_{j=0}^{\infty} j a_j \zeta^{j-1}. \tag{268}$$

Taking the second derivative of the series term by term we have

$$\frac{d^2h}{d\zeta^2} = 2a_2 + 2\cdot 3a_3\zeta + 3\cdot 4a_4\zeta^2 + \cdots = \sum_{j=0}^{\infty}(j+1)(j+2)a_{j+2}\zeta^j. \tag{269}$$

Putting these derivative into the Schrodinger equation (266) we have

$$\sum_{j=0}^{\infty}\left[(j+1)(j+2)a_{j+2} - 2ja_j + (K-1)a_j\right]\zeta^j = 0. \tag{270}$$

From the uniqueness of power series expansions, the coefficient of each power of ζ must vanish

$$(j+1)(j+2)a_{j+2} - 2ja_j + (K-1)a_j = 0. \tag{271}$$

Solving for a_{j+2}, we have

$$a_{j+2} = \frac{(2j+1-K)}{(j+1)(j+2)} a_j. \tag{272}$$

The recursion formula (272) is equivalent to the Schrodinger equation.

Writing $h(\zeta)$ as

$$h(\zeta) = h_{even}(\zeta) + h_{odd}(\zeta) \tag{273}$$

where $h_{even}(\zeta) \equiv a_0 + a_2\zeta^2 + a_4\zeta^4 + \cdots$ is an even function of ζ built on a_0, and $h_{odd}(\zeta) \equiv a_1\zeta + a_3\zeta^3 + a_5\zeta^5 + \cdots$ is an odd function built on a_1.

The condition for K to yield physically acceptable solutions is

$$K = 2n + 1 \tag{274}$$

for some positive integer n. This is equivalent to

$$E_n = (n + \frac{1}{2})\hbar\omega, \text{ for n=0,1,2,....} \tag{275}$$

which is the fundamental quantization condition for the energy levels of the quantum harmonic oscillator.

For the allowed values of K, the recursion formula is

$$a_{j+2} = \frac{-2(n-j)}{(j+1)(j+2)} a_j. \tag{276}$$

For $n = 0$, only one term in the energy series (276) exist, and $a_1 = 0$ (to eliminate h_{odd}). In (276), when $j = 0$, $a_2 = 0$

$$h_0(\zeta) = a_0 \tag{277}$$

and the state function is

$$\psi_0(\zeta) = a_0 e^{-\frac{\zeta^2}{2}}. \tag{278}$$

For $n = 1$, choose $a_0 = 0$, and in (276) when $j = 1$ we find that $a_3 = 0$. We then have

$$h_1(\zeta) = a_1 \zeta \tag{279}$$

and the state function is

$$\psi_1(\zeta) = a_1 \zeta e^{-\frac{\zeta^2}{2}}. \tag{280}$$

For $n = 2, j = 0$ yields $a_2 = -2a_0$, and $j = 2$ gives $a_4 = 0$, so

$$h_2(\zeta) = a_0(1 - 2\zeta^2) \tag{281}$$

and the state function is

$$\psi_2(\zeta) = a_0(1 - 2\zeta^2)e^{-\frac{\zeta^2}{2}}. \tag{282}$$

We can generalize these results, and see that $h_n(\zeta)$ is a polynomial of degree n in ζ, involving only even powers if n is an even integer, and odd powers on if n is an odd integer. Apart from the overall factor (a_0 or a_1), these are polynomials are **Hermite polynomials**, $H_n(\zeta)$. The first 5 Hermite polynomials are

$$H_0 = 1 \tag{283}$$

$$H_1 = 2x \tag{284}$$

$$H_2 = 4x^2 - 2 \tag{285}$$

$$H_3 = 8x^3 - 12x \tag{286}$$

$$H_4 = 16x^4 - 48x^2 + 12 \tag{287}$$

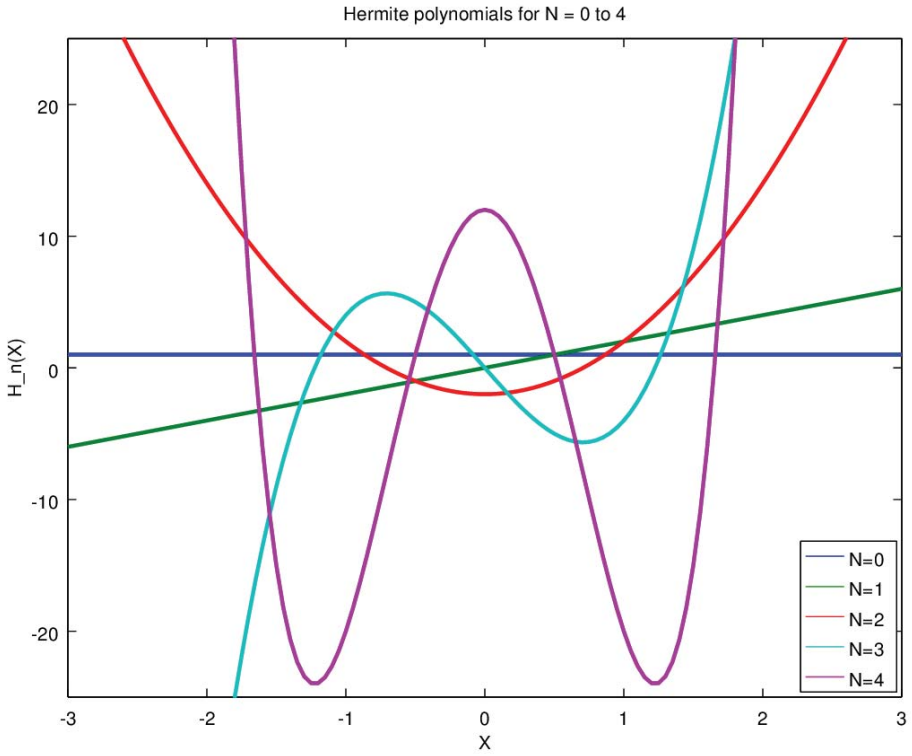

Figure 16: The first 5 Hermite polynomials.

An arbitrary multiplicative factor is chosen so that the coefficient of the highest power of ζ is 2^n. The normalized stationary states for the harmonic oscillator are then

$$\psi_n(x) = \left(\frac{m\omega}{\pi\hbar}\right)^{1/4} \frac{1}{\sqrt{2^n n!}} H_n(\zeta) e^{-\frac{\zeta^2}{2}}. \tag{288}$$

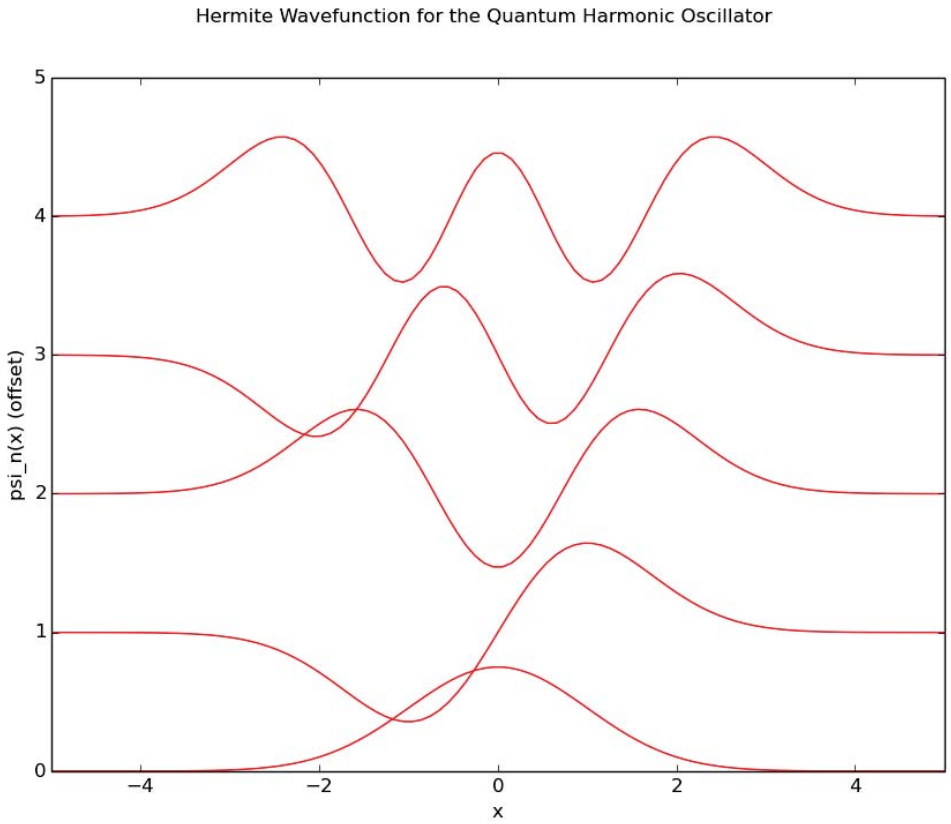

Figure 17: The first 5 Hermite wavefunctions.

The differences between the classical harmonic oscillator and quantum harmonic oscillator are not only the energies (the quantum harmonic oscillator having quantized energies), but there are also differences in their position distributions. For example, the probability of finding the particle outside the classically allowed range (x is greater than the classical amplitude for the energy in question) is not zero, and in all odd states the probability of finding the particle at the center of the potential well is zero. Only for large n do we see some similarities to the classical case.

APPENDIX G

How To Use MEEP

This section describes operations in MEEP such as installing MEEP, defining parameter, seting up geometries, how run MEEP simulations, and create visuals. MEEP can be installed on a Ubuntu computer from the terminal by typing

```
apt-get install meep h5utils
```

The rest of this section assumes MEEP is used on a Ubuntu GNU/Linux operating system.

Scripts written for MEEP must be saved as a *.ctl* file. Users can use text editors, such as *gedit*, to create these scripts. For the example presented here (adopted from the MEEP tutorial found at `http://ab-initio.mit.edu/wiki/index.php`), the file will be called *example.ctl*, and saved in the location Documents/MeepFolder

Before the geometry of the simulation can be defined, the computational cell must be defined. This is the total area of the simulation. The computational cell can be defined by the following command

```
(set!  geometry-lattice (make lattice (size 16 8 no-size)))
```

This command defines the computational area as 16 units in the horizontal (x) direction, and 8 units in the vertical (y) direction. The command `no-size` means that the z dimension is not defined a size, therefore we have defined a 2D geometry.

For this example, lets calculate the field intensity profile in a planar homogeneous waveguide. The geometry of the waveguide can be defined by the following command

```
(set!  geometry (list (make block (center 0 0) (size infinity 1 infinity)
```

```
material(make dielectric(epsilon 12))))))
```

The command `make block` creates a rectangular geometry, `(center 0 0)` defines the rectangle to be centered at the point (0,0), and `(size infinity 1 no-size)` defines a waveguide infinitively long in the x direction, 1 unit in the y direction, and the z direction does not have a defined dimension. Other types of shapes that can be defined are spheres, cylinders, cones, and ellipsoids. More complex geometries are created by overlaying these shapes in a systematic way until the desired geometry is created.

The material is defined as a dielectric material by `material(make dielectric` and the dielectric constant of $\epsilon = 12$ is defined by `(epsilon 12)`. Other material properties such as relative permeability, electric and magnetic conductivity can also be defined.

Sources are defined by the command

```
(set!  sources(list
  (make source
  (src(make continuous-src(frequency 0.15)))
  (component Ez)
  (center -7 0))))
```

This defines a continuous wave source proportional to $\exp(-i\omega t)$, with a frequency = 0.15 which is in units of $c/distance$, and ω is in units of $2\pi c/distance$. The source is located at the point $(-7, 0)$, which is one unit away from the left boundary. This is so that the PML boundary condition does not interfere with the source. The component E_z is chosen as the field component we wish to see. The data written in the corresponding `.h5` file will only be for the E_z component of the field.

We wish to have reflectionless boundaries. We use the *perfectly matched layers* command

```
(set!  pml-layers (list (make pml (thickness 1.0))))
```

with a thickness of 1 unit. The following command discretizes the geometry

```
(set!  resolution 10)
```

This will create 160 grids in the x dimension, and 80 grids in the y dimension. Lastly, we define how long to run the simulation, and what to output with the following command

```
(run-until 200 (at-beginning output-epsilon)(at-end output-efield-z))
```

This means the simulation will run for 200 time steps, and will create two output files. The command `(at-beginning output-epsilon)` will write a file that will show the index profile, or the dielectric profile of the geometry. The command `(at-end output-efield-z)` will create a file that contains the E_z intensity profile data.

To run the MEEP simulation, from the terminal go to the directory where the simulation was saved

```
unix:~$cd Documents/MeepFolder
```

then type the command

```
unix:~/Documents/MeepFolder$ meep example.ctl
```

MEEP outputs simulation results in the HDF5 format. These files can be post-processed by any image processing software. An example of a command that will create a visual from the `.h5` file is

```
unix:~/Documents/MeepFolder$ h5topng -S3 example-eps-000000.00.h5
```

This uses the `h5topng` function, and will create a `.png` file of the geometry and dielectric constant profile. The option `-S3` is a scaling option, which in this case scales the image by 3. The image created by this command is Figure 17

Figure 18: MEEP example.ctl geometry and dielectric constant profile.

An example of a command that will create a visual of the E_z field intensity profile is

```
unix:~/Documents/MeepFolder$ h5topng -S3 -Zc dkbluered -a yarg -A
example-eps-000000.00.h5 example-ez-000200.00.h5
```

The `-Zc dkbluered` option will create a color scale that makes areas of negative field intensity blue, areas where the field intesity is zero white, and areas with positive field intesity values as red. The `-a yarg -A` will overlay the dielectric profile and geometry in light gray. The resulting image of this simulation is

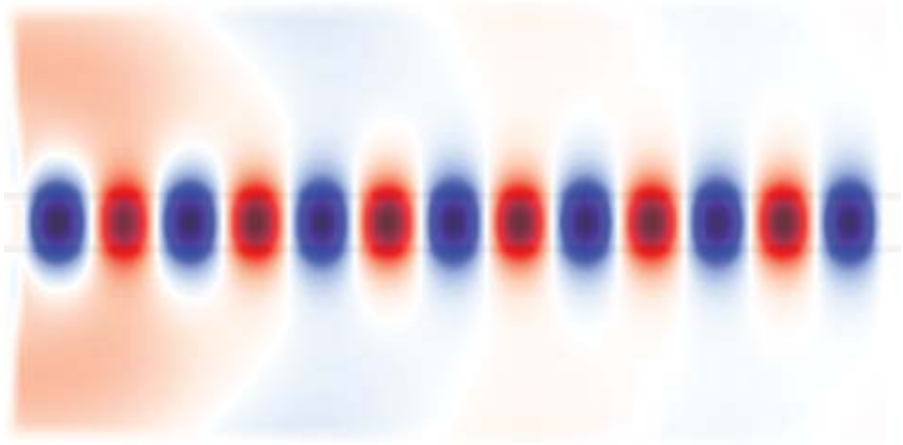

Figure 19: MEEP example.ctl E_z field intensity profile.